CHALMERS

Measurement of ion mobility in dielectric liquids

Master of Science Thesis in Electric Power Engineering

MOHSEN SHAFIEE ZADEH

Department of Materials and Manufacturing Technology
Division of High Voltage Engineering
CHALMERS UNIVERSITY OF TECHNOLOGY
Göteborg, Sweden, 2011

Report No. 66/2011

Measurement of ion mobility in dielectric liquids

by

Mohsen Shafiee zadeh

Diploma work No. 66/2011
at Department of Materials and Manufacturing Technology
CHALMERS UNIVERSITY OF TECHNOLOGY
Gothenburg, Sweden

Diploma work in the Master program Electric Power Engineering

Performed at: ABB Corporate Research
SE-721 78 Västerås, Sweden

Supervisor(s): Dr. Joachim Schiessling
ABB Corporate Research
SE-721 78 Västerås, Sweden

Examiner: Professor Stanislaw Gubanski
Department of Materials and Manufacturing Technology
Chalmers University of Technology, SE - 412 96 Gothenburg

Measurement of ion mobility in dielectric liquids
MOHSEN. SHAFIEE ZADEH

© MOHSEN. SHAFIEE ZADEH, 2011.

Diploma work no 66/2011
Department of Materials and Manufacturing Technology
Chalmers University of Technology
SE-412 96 Gothenburg
Sweden
Telephone + 46 (0)31-772 1000

Chalmers Reproservice
Gothenburg, Sweden 2011

Measurement of ion mobility in dielectric liquids

MOHSEN. SHAFIEE ZADEH
Department of Materials and Manufacturing Technology
Division of High Voltage Engineering
Chalmers University of Technology

Abstract:

Rising energy demand and at the same time global effort to reduce greenhouse gases are strong pushes for harvesting renewable energy sources in remote areas far away from consumption centers. Ultra High Voltage Direct Current is a highly efficient way to transfer bulk power over long distances. One key component for the reliable energy transfer in this technology is HVDC converter transformer. The insulation system of HVDC converter transformers, which basically consists of oil and paper/pressboard with different dielectric properties, needs to withstand AC and DC stresses. In particular for the UHVDC application the transient phenomenon of electric stress due to space charges needs to be further understood in order to design an insulation system for safe operation during long service life time. A physical model commonly called the ion drift model describes space charge accumulation on solid-liquid interface by ion transport in liquid. One important parameter in this model is the ion mobility.

An investigation was made to evaluate the experimental set up for ion mobility measurement in COMSOL Multiphysics®. Charge transport, electric field distributions and current curves were studied in a bulk of oil under dc voltage application. After analyzing the simulation result decision concerning the set-up type was made by having two factors in mind: accuracy and large enough signal to determine the mobility. Based on the physical picture of the ion movement in the transformer oil obtained by the numerical calculation, the plane parallel electrode geometry had been chosen for experiment.

The evolution of instrument and software for data acquisition during the experiment enabled us to get the desired data. The measurements were carried out for two types of dielectric liquid: mineral oil and natural ester oil. By obtaining information on the time of flight from the current curves, the mobility of ions in positive and negative voltage application for the respective liquids were determined. For mineral oil the measured mobility was around $2.61 \pm 0.175 \times 10^{-9}\ \frac{\mathrm{m}^2}{\mathrm{Vs}}$ and for natural ester oil was $1.67 \pm 0.18 \times 10^{-10}\ \frac{\mathrm{m}^2}{\mathrm{Vs}}$.

Key Words: UHVDC, UHVDC converter transformer, Ion drift model, Ion mobility, transformer oil

Preface

In this master project measurement had been carried out to obtain mobility of ions in positive and negative voltage application in dielectric liquids. The study was carried out from March 2011 to August 2011 and was a co-operation between ABB corporate research Sweden and the Division of High voltage engineering at Chalmers University of Technology, Sweden.

First and foremost I would like to thank my supervisor at ABB corporate research Joachim Schiessling for his support, patience and guidance. I have learned a lot from you during the thesis work. Also I want to thank Olof Hjortstam for fruitful discussion every time when I met him. I am very grateful for valuable comments I received throughout the project from Uno Gäfvert.

Thanks also to Prof. Stanislaw Gubanski for his help and being my examiner at Chalmers University. Furthermore, thanks to Assoc. Prof. Yuriy Serdyuk for continuous help.

I would like to give my gratitude to Leif A Pettersson and all the staff at ABB CRC, Västerås, especially ELD group, for their support and for providing a good working climate. My acknowledgment also goes to all my friends for providing good atmosphere during the study.

Last, but defiantly not least, I want to thank my family for their support and encouragements.

Göteborg September 2011
Mohsen Shafiee zadeh

TABLE OF CONTENTS

1 INTRODUCTION 1

2 PHYSICAL MODEL 2

2.1 CHARGE CARRIERS IN TRANSFORMER OIL 2
2.2 PHENOMENA ON OIL-METAL INTERFACES 6
2.2.1 ELECTRICAL DOUBLE LAYER 6
2.2.2 CHARGE INJECTION 7
2.3 MOBILITY OF IONS 8
2.3.1 APPARENT MOBILITY 9
2.3.1.1 INSTABILITY IN TRANSIENT CONDITION OF UNIPOLAR INJECTION 10

3 COMPUTER MODEL AND SIMULATIONS RESULTS: 12

3.1 SIMULATION RESULTS 12
3.1.1 CASE A – LOW CONDUCTIVE OIL, Σ = 10-13 S/M, NO INJECTION 13
3.1.1 CASE A – LOW CONDUCTIVE OIL, Σ = 10-13 S/M, NO INJECTION 26

4 EXPERIMENTAL 32

4.1 EXPERIMENTAL SET-UP 33
4.1.1 MEASURING INSTRUMENTS 36
4.1.2 CLEANING PROCEDURE OF TEST CELL 36
4.2 ION MOBILITY MEASUREMENT 36
4.2.1 SINGLE POLARITY METHOD 36
4.2.2 POLARITY REVERSAL METHOD 42
4.3 RESISTIVITY MEASUREMENTS 50
4.4 DISCUSSION 52

5 CONCLUSIONS AND FUTURE WORK 57

5.1 CONCLUSIONS 57
5.2 FUTURE WORK 57

6 REFERENCES 58

7 APPENDIX A 60

7.1 TABLE OF EXPERIMENT RESULTS 60
7.2 KINEMATIC VISCOSITY 62

1 INTRODUCTION

Enormous increase in electricity consumption worldwide needs to find and use renewable energy sources. Recently a global effort for developing these relatively new sources of energy has been driven by their advantages to minimize the global warming and environmental impact. Utilizing renewable energy sources require transporting bulk energy from generation centers far away from the consumption locations. High Voltage Direct Current (HVDC) is an advanced technology suited quite well for this purpose.

HVDC transmission system has a better energy efficiency comparing to High Voltage Alternating Current (HVAC) over a long distances. HVDC converter transformer is a key component in this system. Increasing demand in voltage and power rating and also higher material cost push manufacturers for building more compact and reliable transformers. To tackle challenges in designing reliable transformer a deep knowledge of field behavior is a necessity, which can be achieved by coupling numerical simulations and experimental investigation.

One of the aspects in designing this type of transformer is an electrical insulation system since it faces both ac/dc stresses. The insulation system of UHVDC transformers basically consists of solid pressboard, and liquid transformer oil. Large volumes of the oil are subjected to DC voltage in UHVDC converter transformer demanding high electrical and thermal performance. The transformer oil besides being dielectric has a task of cooling the transformer.

A physical ion drift model that can describe space charge accumulation at pressboard barriers due to ion dissociation and migration in the oil driven by the constant electric field is commonly called the ion drift model. The ion drift model can be implemented in COMSOL Multiphysics for numerical calculations. One important parameter in the model is the ion mobility. The aim of this thesis is to measure the mobility of ions for positive and negative voltage application in two types of transformer oil: mineral and ester based oils. Mineral oil is nowadays an important insulant in high capacity power transformers.

In chapter two the physics of charge generation and movement in the oil is discussed. In the third chapter physical model implemented in COMSOL Multiphysics® and the simulation results are provided. The fourth chapter provides information about experimental set-up and discusses the obtained results. The fifth chapter presents conclusion and indication for future work.

2 PHYSICAL MODEL

2.1 Charge carriers in transformer oil

To design a reliable HVDC converter transformer the behavior of dc stressed transformer oil need to be understood. The studies in transformer oil with the resistivity near to $1 \times 10^{13}\,\Omega\mathrm{m}$ show that a simple model based on the ions pair dissociation in the bulk of oil can predict the main feature of the steady state field distribution [1].

The insulation system of the HVDC converter transformer which basically consists of mineral oil and pressboard is subjected to both dc/ac stresses, so the insulation system should be able to handle these stresses. HVDC equipment will be exposed not only constant DC but also sudden voltage change at turn on, turn off and DC polarity reversal. The DC polarity reversal can be very severe for HVDC insulation since accumulated charges on the solid insulation can be superimposed to the applied field, which leads appearance of a strong electric field in a certain place of the equipment [2]. The Laplacian AC field can be accurately calculated with standard numerical methods but because of space charge effects the method is less straightforward for DC field calculation [3].

In the transformer oil, which is a weak electrolyte, dissociation of the ionic pairs generates free ions and, on the other hand, ionic pairs are formed by recombination of free ions [5]. Electric conduction of the oil is therefore due to the ions in the liquid (residual conduction) or due to charges injected from the electrodes (injection) [6].

The ions can be transported by applying electric field and also recombine to form neutral molecules. This is in accordance with Bjerrum's, [7] theory which predicts that only a minor number of the ion pairs dissociates. The majority of the ions in a weak electrolyte are associated to ion pairs and just a few can dissociate to free ions [8]. The ion-ion and ion-metal associations are responsible for high resistance in weakly polar or non-polar liquids at zero fields. These associations explain the large increase in current density or electric losses in high electric field which leads to field enhanced dissociation.

Charge carriers in low permittivity ($\varepsilon_r < 5$) liquids are produced in the bulk of liquid or at metal-liquid interface in a two step process: ionic dipole formation and then separation of these charges:

$$R_1\,R_2 \underset{K_2}{\overset{K_1}{\rightleftarrows}} R_1^+R_2^- \underset{K_R}{\overset{K_D}{\rightleftarrows}} R_1^+ + R_2^- \tag{1}$$

Where $R_1^+R_2^-$ is the neutral ion pair formed from two ions: R_1 and R_2 .The K_1 ,K_2, K_D , K_R are kinetic rate constants, out of which just dissociation constant K_D is a field dependent. The recombination constant K_R is field invariant.

The same explanation can be used for injection of charge carriers by a metallic electrode: creation of a charge carries and then extraction of ions from the image-force section.

In the transformer oil, similarly as in pure cyclohexane, at high electric field the conduction is due to unipolar injection and in lower fields it is due to ions created by both dissociation and injection [9].

Free ions are continuously being generated from the dissociation of ionic pairs and, conversely, ionic pairs are formed by the recombination of ions. The rate of generation of positive and negative ions in the bulk of the fluid is given by the rate equation [10]:

$$\frac{\partial \mathrm{p}}{\partial \mathrm{t}} = \frac{\partial \mathrm{n}}{\partial \mathrm{t}} = \mathrm{k_D c} - \mathrm{k_R pn} \tag{2}$$

Here p and n are positive and negative ion density respectively and c is ion pair density. The densities of negative and positive ions present in transformer oil are much less than the concentration of ionic pairs [5] p<<c, n<<c, and the density of ionic pairs c can be taken as a constant.

Onsager theory [11] describes the dependence of the conductivity in a weak electrolyte on an applied electric field. In his theory the liquid contain a certain concentration of ion-pairs, c ($1/m^3$) and certain amount of equal negative and positive ions, $\mathrm{n}\left(\frac{1}{m^3}\right), p\left(\frac{1}{m^3}\right)$. Two kinetic constants control the rate of ion pair dissociation and recombination of free ions. The dissociation constant, $\mathrm{k_D}$ is given by:

$$k_D = k_D^0 F(b) = k_D^0 \frac{I_1(4b)}{2b} \tag{3}$$

$$b = \frac{\frac{q^2}{8\pi\varepsilon_0\varepsilon_r KT}}{(\frac{q}{4\pi\varepsilon_0\varepsilon_r |E|})^{0.5}} \tag{4}$$

Here, $\mathrm{I_1}$ is the modified Bessel function of first kind and order one, K is a Boltzmann constant, q is the elementary charge and T is absolute temperature. In the limit,$E \to 0$, dissociation constant has a constant value k_D^0 .

The electric field dependence of k_D leads to increase of the free ions concentration and consequently the liquid conductivity in higher electric fields [12].

The recombination constant, $\mathrm{k_R}$ can be calculated using Langevin approximation:

$$k_R = \frac{q(\mu_p + \mu_n)}{\varepsilon_0\varepsilon_r} \tag{5}$$

Where μ_p and μ_n are positive and negative ion mobility respectively. In thermal equilibrium and no applied electric field:

$$\mathrm{c}k_\mathrm{D}^0 = \mathrm{n_0}^2 k_\mathrm{R} \tag{6}$$

The equilibrium density of charge carriers can be calculated from conductivity σ of the liquid:

$$n_0 = \frac{\sigma}{q(\mu_p + \mu_n)} \tag{7}$$

The initial conductivity of the oil has a strong influence on the time variation of the electric field under dc stress [5].

If an external electric field is applied, the equilibrium conditions (6)-(7) are not valid anymore. Conductivity of the dielectric is not constant and in general by ignoring diffusion can be calculated by:

$$\sigma = \mathrm{q}(\mu_\mathrm{p}\mathrm{p} - \mu_\mathrm{n}\mathrm{n}) \tag{8}$$

At t=0, conductivity is a constant value everywhere at bulk.

In DC application space charge effect cannot be excluded and the conductivities can vary orders of magnitude during test and service and this make the modeling more complex because bulk space charge effect can't be taken into account in simple type of the conductivity model [8].
In ionic conduction of liquids according to Thomson [13] model two process are involved, dissociation of neutral molecule and the recombination of charge carriers [14].The assumption that an infinite source of ionizable species generates charge carriers in the bulk of liquid at the fixed rate could be incorrect. The fact that oil conductivity decrease for the time shortly after voltage application is proved that the rate of charge carrier generation is reduced with increasing time of voltage application[8].
Charge carriers in the bulk of the fluid are subjected to electrostatic forces and move towards the electrodes having opposite signs. The drift velocities of charge carriers are defined by their mobilities and the electric field strength:

$$\vec{w}_{p,n} = \mu_{p,n}\vec{E} \tag{9}$$

By knowing drift velocity, $\vec{w}_{p,n}$ obtained from the time needed for an ion to reach the opposite electrode, the mobility of ions can be obtained for that specific electric field.
The magnitudes of the diffusive fluxes due to not equal concentration of ions in different points at bulk of liquid, are proportional to the gradients of the ions densities: $-D_p \nabla p$ for positive, and $-D_n \nabla n$ for negative ions. Diffusion coefficients $D_{p,n}$ are found using Einstein's relation:

$$D_{p,n} = \frac{kT}{q}\mu_{p,n} \tag{10}$$

The diffusion coefficient, D, of a particle with a radius of R related to the viscosity **η** by the Stokes-Einstein equation:

$$D = \frac{k_B T}{C\pi\eta R} \tag{11}$$

Where k_B is a Boltzmann constant, T the temperature and C is a constant which shows the interaction type between the atoms and molecules of the liquid and particles. If a few layers of the liquid are tightly bound to the particle, sticking condition, the constant is C=6 and if the contact is minimal, slipping condition, the constant is C=4. The diffusion coefficient for the ions is proportional to the mobility:

$$D_{ion} = \frac{k_B T \mu_{ion}}{q} \tag{12}$$

Combining above equation gives the Stokes formula of the ion mobility:

$$\mu_{ion} = \frac{q}{C\pi\eta R} \tag{13}$$

From above equation Walden's rule can obtained:

$$\mu_{ion} \times \eta = \text{const.} \tag{14}$$

The ionic radius R can be obtained from the measured mobility. Deviations from the Walden's rule have however been observed [15].
Moving of spherical ions with a R radius in a liquid with viscosity of η causes a laminar flow of the liquid around the ion. The viscous force which is given by Stokes law is counter balanced the electric force, qE.

$$\mathrm{F} = 6\pi\eta\mathrm{R}\nu \tag{15}$$

Where ν is an ionic velocity. Walden's rule gives the relation between the mobility μ and the liquid viscosity [4]:

$$\mu\eta = \frac{\mathrm{q}}{6\pi\mathrm{R}} \tag{16}$$

Equation (2) can be extended into equations considering ionic drift and diffusion, which describes transport of charges through the bulk of fluid accounting for sources and sinks of charges:

$$\frac{\partial \mathrm{p}}{\partial \mathrm{t}} + \nabla\left(\mu_\mathrm{p}\vec{\mathrm{E}}\mathrm{p} - \mathrm{D}_\mathrm{p}\nabla\mathrm{p}\right) = \mathrm{S} \tag{17}$$

$$\frac{\partial n}{\partial t} - \nabla\left(\mu_n\vec{E}n + D_n\nabla n\right) = S \tag{18}$$

Right side of equation (17) and (18) has two parts: generation and recombination of ions:

$$S = \mathrm{k}_\mathrm{D}^0\mathrm{cF(E)} - \mathrm{k}_\mathrm{R}\mathrm{pn} \tag{19}$$

The ionic current density between electrodes is defined by the total ionic fluxes:

$$\vec{J_p} = q\left(\mu_p\vec{E}p - D_p\nabla p\right), \quad \vec{J_n} = -q\left(\mu_n\vec{E}n + D_n\nabla n\right), \quad \vec{J}_{ion} = \vec{J}_p + \vec{J}_n \tag{20}$$

The current density is proportional to the free ion concentration calculated from the conductivity of the liquid, electric field and the charge mobility ignoring diffusion and injection [16]. All the free charges are moving in the dielectric by applying electric field, contributing to the measured current in external circuit. The total ionic current in the external circuit can be found by integrating the current density $\vec{J}_{ion}$ over the cross-section perpendicular to the direction of the current (e.g. on one of the electrodes).
Displacement current $\vec{J}_{Displacement}$ associated to the change of the electric field can be calculated by integration on the electrode surface. The electric field change is due to applying a voltage to the high voltage electrode and moving of the ions.

$$-\mathrm{J}_\mathrm{D} = \frac{\partial \mathrm{D}}{\partial \mathrm{t}} = \varepsilon_\mathrm{r}\varepsilon_0\frac{\partial \mathrm{E}}{\partial \mathrm{t}} = -\mathrm{J}_\mathrm{D}^{\mathrm{V\ ramp\ up}} - \mathrm{J}_\mathrm{D}^{\mathrm{ion\ movement}} \tag{21}$$

Displacement current has a contribution from two phenomena:

A) Moving charges:

Moving charges towards the opposite electrodes cause the change in the electric field and as far as there is electric field variation we have displacement current.

B) Voltage turn on:

A sudden increase of applied voltage from zero to its maximum value causes the electric field to change and consequently displacement current will be generated.
The total current is the sum of ionic current and displacement current.

$$\vec{J}_{tot} = \vec{J}_{ion} + \vec{J}_{Displacement} \tag{22}$$

A quasistatic current is reached after a long time (up to 20 hours or more) in non-polar liquids when a dc voltage is applied between plane parallel electrodes. The current curve gives overall information and it is not possible to find out which part is due to the residual conduction due to the ions in the liquids or ions created by the electrode, injection. More information about mobility of the ions, origin of the ions can be obtained by studying the transient of the conduction [6].
In order to investigate charge injection and transport in dielectric liquids the charge continuity equations and Poisson's equation for the electric potential should always be satisfied [17].

$$\nabla.(\varepsilon_0\varepsilon_r\nabla\emptyset) = -q(p-n) \quad , \quad \nabla.(-\varepsilon\nabla\emptyset) = \rho_+ + \rho_- \quad , \; \mathrm{E} = -\nabla\emptyset \tag{23}$$

Here, the electric potential is the function of space co-ordinates Φ = Φ(x,y,z) with known magnitudes on the boundaries (e.g. electrodes, walls) and space charge is $q(p-n)$.

2.2 Phenomena on Oil-Metal Interfaces

Up to now, processes in the bulk of the fluid were described. The understanding of charge transport and injection properties is essential for understanding the pre-breakdown phenomena in dielectric liquids [16].
As it has been mentioned in section 2.1, that separation of charges generated and drifting in oil due to the applied field leads to formation of electrical double layers on oil-metal interfaces. The specific adsorption phenomenon at the contact between a liquid and a solid leads to the development of an electrical double layer [18].

2.2.1 Electrical Double Layer

There is an electrical double layer at any solid/liquid interface which the liquid layer with opposite sign of the solid wall comprise of an inner and outer part, the diffuse layer, with length equal to the Debye length:

$$\mathrm{L_D} = [\frac{\varepsilon_0\ \varepsilon_\mathrm{r}}{2\mathrm{q}_0}\frac{\mu\mathrm{T}}{\mathrm{e}}]^{1/2} \tag{24}$$

Typical magnitude of L_D for transformer oil is of order of tens of micrometers. Double layer shows the pre- existence of the unipolar charged layer at the vicinity of each electrode and depending to its polarity the layer tend to move towards the opposite electrode or will be blocked against the electrode [19].
In the metal-liquid interface a surface of metal has an excessive number of free electrons which attract some positive ions on the oil side which will be accumulated on the interface, and thus the oil will be negatively charged, Figure 1.

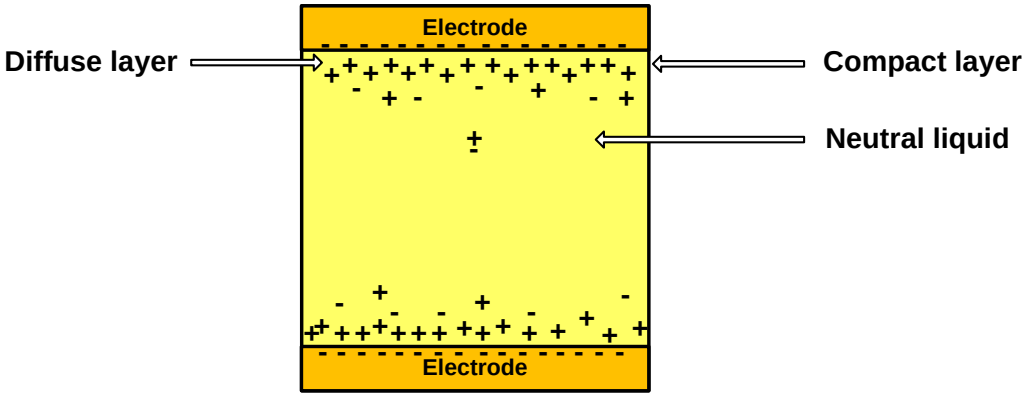

Figure 1. Electrical double layer at metal/liquid interface

2.2.2 Charge injection

The accumulation of charges with opposite sign of the electrode, preferential adsorption, leads to injection of charges having the same sign as the electrode to the bulk of liquid. The injection in non-polar liquids occurs in two steps: ions created on the electrode and then injected to the liquid by overcoming the image-force barrier [20].
The injected charges are identical to the corresponding ions created by dissociation in the bulk of the liquid. The injected charge density due to escape of ions from the double layer due to Schottky emission is equal to:

$$n_{inj} = n_0 F_i(b) = \frac{n_0}{2bK_1(2b)} = \frac{\sigma}{q(\mu_p + \mu_n).2bK_1(2b)} \quad (25)$$

Where K_1 is the modified Bessel function of the second kind and order one; the argument b should be calculated at the injecting surface. At low electric field, below 10^6 V/m, the function of bulk generation and function of the ion injection are field independent since they are equal to one.
It is expected that by increasing the oil conductivity the effect of injection would be seen. Experimental conditions observed for the low field (0.16 MV/m) shows that liquid bulk rather than solid-liquid interface is the charge source [1]. Denat, et al showed in [6] that in hydrocarbons with dissolved electrolyte, which has a resistivity less than $2 \times 10^{12} \Omega m$, it is necessary to observe carrier injection from the electrodes. The injected current can be defined by knowing the density of injected charges:

$$\vec{j}_{inj} = q\mu n_{inj} \vec{E}_{sur} \quad (26)$$

Where, $\vec{E}_{sur}$ is the electric field at the injecting surface.
Unipolar injection in a motionless medium of a perfect insulator under a step voltage can be categorized in two groups:

(a) Transient space charge limited current (TSCLC)

The current is limited by the space charge in this case. By neglecting diffusion and considering injector is able to inject an infinitive volumic space charge $q_i = \infty$ for any time ≥ 0 , the electric field at the injector will remain zero. The analytical expressions for the

current density and the electric field up to the time of the flight t = t_1 equal to the time when of the first injected charges reaches to the opposite electrode, can be calculated.
The arrival of the first charges from the injector to the collector can be seen as a cusp in the current density Figure 2. For t > t_1 the current decreases and tends to its stationary value.
Experimentally the current curve at the maximum is rounded due to the diffusion in liquids and solid.

(b)Transient electrode limited current (TELC)

In this case the current is limited by the emission of carriers and not by the space charge. The strength of the injection can be characterized by the number C_i

$$C_i = q_i L^2/\varepsilon V \tag{27}$$

Here ε is a permittivity of the medium; V is the applied voltage, L gap distance, q_i is a space charge at the injector.

- Strong injection: $5 < C_i < \infty$ ($C_i = \infty$ is corresponds to TSCLC)
- Medium injection: $0.2 < C_i < 5$ and
- Weak injection : $0 < C_i < 0.2$

Charges may pre-exist near collector and injector for particular case of liquids and contribute to instabilities and transient current [19].
In the transient case of simple oil gap the dissociation behavior normally dominates over the charge injection effects [8].
The field level needed for streamer initiation in transformer oil is typically greater than 2.0 MV/cm.

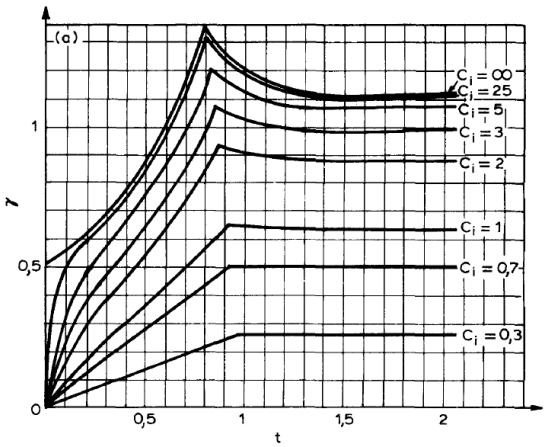

Figure 2. Time variation for the transient current density for various C_i-[21]

2.3 Mobility of ions

Ions in the transformer oil are atoms or molecules which number of electrons and protons are not equal. The ion is negatively charged if number of electron is more than the proton and vice versa. Electron affinity of these different types of ions is not the same so some of them attract electron faster. Different type of ions can have different mobility and so more equations are needed in simulation for different type of ions if this hypothesis is true.
The mobility of the ions in dielectric liquids has been studied experimentally and theoretically for a long time [15]. The studies before 1970 for hydrocarbons and related compounds have

been summarized by Adamczewski [22]. The mobility of ions is an important parameter to understanding the process of electric breakdown in dielectric liquids such as hydrocarbons [23] and simulation of electric field distribution of HVDC converter transformers.
Ion mobility can be measured directly from the time needed for ions to drift between parallel plate electrodes [23]. The mobility value can be calculated according to formula (9):

$$\mu_{p,n} = \frac{\vec{w}_{p,n}}{\vec{E}} = \frac{d^2}{Vt} \tag{28}$$

Where d is a gap distance, t is the time of flight or transit time of ions from one electrode to the opposite electrode and V is an applied voltage. To calculate the average mobility of charge carriers from the transient current followed by the step voltage one should be careful to avoid electrohydrodynamic (EHD) instabilities by applying low voltages in a small distance gap [8].

2.3.1 Apparent mobility

The true ion mobility is the mobility of the ions due to the application of the voltage (electric field). If the molecules of the liquids are moving as well, a component can be added to the mobility of charge carrier due to the general motion of the fluid. The measured mobility will therefore be an “apparent mobility”. The effect of the EHD motion should be considered in the experimental measurements of the ion mobility.
Since the 17th century it has been known that forces applied on an insulating dielectric liquid could produce various hydrodynamical effects. EHD is a field of electrodynamics which deals with movement of dielectric fluids due to electric force. Two types of electric forces are the reason of permanent fluid motion: Coulomb force $q\vec{E}$ and where $\vec{E}$ is the electric field acting on charges with density q and dielectric force of density $-(\frac{E^2}{2})\nabla\varepsilon$ where $\nabla\varepsilon$ is the permittivity gradient that is equal to zero in isothermal and homogeneous fluid. EHD can be investigated in two ways depending on whether the force is restricted to the interface or applied to the volume. The strong nonlinear coupling between motion and force make EHD a difficult subject.
Space charge in liquids can appeared by different ways in liquids. Bulk charges can originate from weak but nonzero conductivity. Gradient of conductivity induced by temperature gradients also results in space charges. Charge injection is dominant process of space charge formation in fluids. In highly resistive liquids the injected current strongly dominates over the residual conduction current.
The Maxwell equations in the quasi electros static limit where magnetic field is negligible, reduced to:

$$\nabla \times \vec{E} = 0 \tag{29}$$

$$\nabla . \vec{E} = \frac{q}{\varepsilon} \tag{30}$$

$$\frac{\partial q}{\partial t} + \nabla . \vec{j} = 0 \tag{31}$$

Where $\vec{E}$ is the electric field, q is the charge, j is the current density and ε is liquid permittivity. The current density in unipolar injection by neglecting diffusion current can be obtained by:

$$\vec{j} = q\mu\vec{E} + q\vec{u} \quad (32)$$

Where $\vec{u}$ is the velocity, $q\mu\vec{E}$ is the conduction current density and $q\vec{u}$ is the convective current related to the convection of charges by the fluid velocity.
Assuming the liquid to be isothermal and incompressible, the Navier-Stokes expresses the conservation of mass and momentum:

$$\nabla.\vec{u} = 0 \quad (33)$$

$$\rho\left[\frac{\partial\vec{u}}{\partial t} + \vec{u}.\nabla\vec{u}\right] = -\nabla p_1 + \eta\nabla^2\vec{u} - \rho g\vec{\imath}_z + \vec{f}_e \quad (34)$$

Here ρ is the mass density, η is the dynamic viscosity, p_1 is the pressure, $\vec{f}_e$ is the density of the electric force and $\vec{\imath}_z$ is the vertical unit vector.
The motion less solution for unipolar injection for symmetry geometry considering that the uniform density of injected charges, is equal to $\vec{u} = 0$. The instability problem is then the condition that the solution $\vec{u} = 0$ destabilized.
The charge distribution is potentially unstable because of decrease of charge density from the injector to the collector due to Coulomb repulsion, so the instability can be determined as appearing under condition that Coulomb force overcomes the viscous friction. The electric force cannot overcome the viscous friction for low enough voltages [24].

2.3.1.1 Instability in transient condition of unipolar injection

The transient current method was first used to obtain charge carriers mobility. By applying a step voltage, the resulting current will increase up to the maximum in a transient regime which is the arrival of the first injected charges to the collector. By knowing the transit time the mobility can be calculated if the liquid is at the rest. In a strong enough injection or large enough applied voltage before the first injected ions reaching to the opposite electrode a motion sets in, which leads to acceleration of charge transition and which give apparent mobility μ_a higher than the true mobility. In general, μ_a increases with voltage, Figure 3.

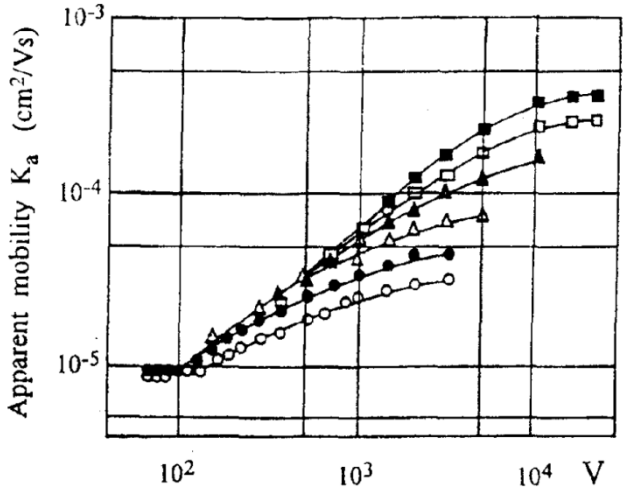

Figure 3. Transient strong unipolar injection in a polychlorobiphenyl variation of the apparent mobility K_a as a function of step voltage for different electrode spacing [24]

Ostroumov [25] analysis showed that different hydrodynamic regimes can be formed, for example laminar flow and then turbulent flow at high electric fields.

Electrohydro-dynamic mobility is equal to:

$$\mu_H = \sqrt{\varepsilon/\rho} \tag{35}$$

Here ρ is a volumic mass of the fluid. In viscous liquids transient apparent mobility can reach to the much higher values than true mobility even for weak injection [19].
The mobility measurement of unknown negative ions in n-hexane as a function of the applied electric filed shows no dependence between mobility and electric field up to $1.5*10^7$ V/m which is the laminar manner movement of the ions. The transition to the turbulent movement is given by the Reynolds number, R_e:

$$R_e = \frac{vl}{\kappa} \tag{36}$$

Where, v is the velocity, l denotes the characteristic length and κ is kinematic viscosity [15].
An apparent mobility larger by order of magnitudes than ionic (true) mobility can be measured in liquids of high M numbers (M is the ratio of the EHD mobility to a true mobility,$M = \frac{\sqrt{\varepsilon/\rho}}{\mu}$) generally viscous liquids. According to the experiment results Figure 4, the EHD motion happens only after a delay time, t_r

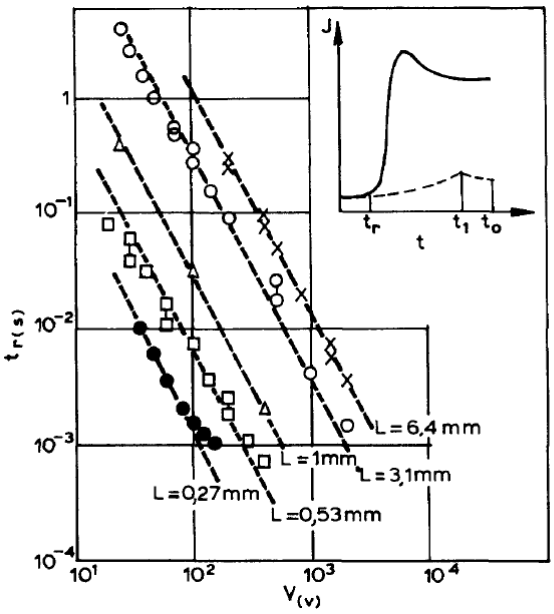

Figure 4. Delay time t_r for the appearance of the instability vs voltage (deionized nitrobenzene) TSCLC (dashed line) and the current with EHD motion [26]

3 COMPUTER MODEL AND SIMULATIONS RESULTS:

In order to plan experimental set-up, one efficient way is computer simulation. The software for computer model should be able to solve multiphysics problem. Ion drift model implemented in COMSOL Multiphysics® v. 3.5a is an appropriate choice for solving space and time dependent and strongly non-linear equations.

Two main options for the mobility measurement set-up were considered at the very beginning stage: a plain parallel electrode system and a wire in coaxial cylinder electrode system. The choice of the experiment set-up should be done by having in mind the following factors:

- It should be possible to distinguish ion mobility in positive and negative voltage application.
- Large enough output signal to calculate the mobility value.

The initial idea to distinguish between ion mobility for respective set-ups was:

I) Covering one electrode with an insulation sheet in plain parallel electrodes system which causes ions accumulation on insulation surface. Voltage reversal will force to move the ions towards the opposite electrode.

The reason for putting insulating sheet on the electrode surface was to prevent ion neutralization on the electrode surface. Further literature study showed that ions are accumulating on the bare electrode surface. In fact a reservoir of undischarged ions should be at electrode surface if electrodes are blocking and by applying the reversing voltage polarity charges will be injected from this reservoir [27].

Moreover putting the insulating paper sheet on the electrode makes simulation and analysis difficult since we do not have detail information on what exactly happening at insulation and oil interface; e.g. how many of the ions will go inside the paper and become trapped there or can they be injected from the insulation. How tight the ions stick to the paper or are they lose enough to be injected to the oil or not.

Previous studies showed that covering electrode with material with lower permittivity than oil would eliminate the image force injection. Covered or uncovered electrode will leads to the same results for electric field in a certain point of the stressed gap [1].

II) Cylindrical electrodes (Thin wire inside a cylindrical electrode)

By applying voltage to thin wire, field enhanced ion pairs dissociation will happen and ions will moves towards the cylindrical electrode. The sign of the ions depend on the sign of the voltage applied to the wire.

3.1 Simulation Results

Charge transfer through the bulk of oil in y-axis direction between two plain parallel electrodes, had been studied in this chapter.

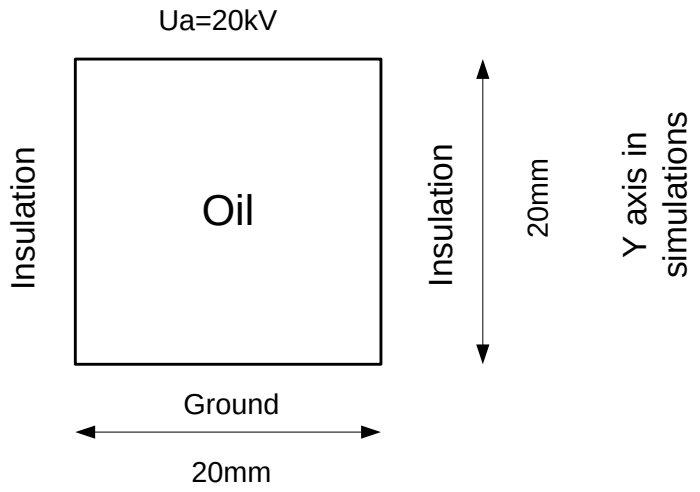

Figure 5. Dimensions, boundary condition used in the simulation

Initial simulations were carried out in COMSOL Multiphysics® v. 3.5a for the oil gap between two bare plain electrodes without considering the effect of charge injection from the metallic surfaces. In the next step, charge injection was implemented on the cathode surface for negative ions. Previous studies showed that negative ion injection is a dominant type of injection [5]. Analyzing the results was expected to give hints for the next steps of the simulation and the experiments.

3.1.1 Case A – Low conductive oil, σ = 10^{-13} S/m, no injection, $\mu_- = \mu_+ = 1e^{-9}\ m^2/Vs$

The 20 mm oil gap presented in Figure 5, was subjected to $10^6\ \mathrm{V/m}$ electric field by applying 20 kV to high voltage electrode. Ions generated in the bulk of oil are transported through the gap where the recombination takes place. Negative ions are moving towards the anode and positive ions moving towards the cathode. The mobility of positive and negative ions was selected equal to $10^{-9}\frac{m^2}{Vs}$.

The voltage reaches to 20kV after 1 second. The function of voltage application needs to be in exponential format otherwise it will cause a problem in numerical calculation.

The results of the simulations are presented as linear plots for different quantities at different time instances by selecting an arbitrary vertical line through the bulk of oil. The origin of the horizontal axis corresponds to the surface of the cathode (lower electrode).

The steady state condition is the time that there is no more change in ion distribution which is around 30 second. Ion concentration in the oil gap decrease at longer times due to the sweep out effect. The outflow boundary condition on the electrode surface leads to reduction of concentration on electrode surface.

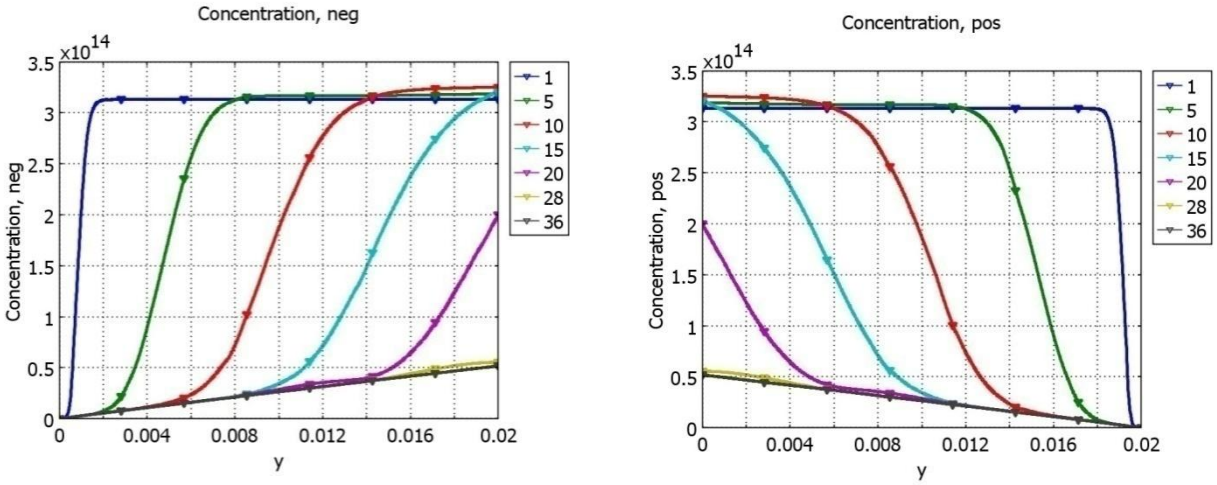

Figure 6. Time variation of the ions concentration.

As seen in Figure 6, the concentration of positive and negative ions have a similar shape which shows the movement of ions generated in the bulk of oil due to field enhanced dissociation or thermal generation towards the opposite sign electrodes. The equilibrium ion density is about $3.1 \times 10^{14}\ \frac{ion}{m^3}$ which can be seen at time t = 1s. Ions with opposite sign will be accumulated on the electrode surface which can be seen in seconds 1, 5, 10, and 15. At longer times the amount of charges available in the gap decreases due to sweeping out effect and their losses at the electrodes surface because of outflow boundary condition used on the electrode surface become dominating. This leads to the reduction of space charge density in the boundary layers (curve 28 to 36 second) and finally a steady state is reached around 30 s and no more changes in charge distribution can be observed at longer times.
The final value of the concentration on the electrode surface decreased from the equilibrium density of $3.1 \times 10^{14}\ \frac{ion}{m^3}$ to $0.5 \times 10^{14}\ \frac{ion}{m^3}$ due to outflow boundary condition. The concentration of the ions with the same sign as that of the electrodes is forced to zero due to no injecting boundary condition.

After reaching the steady state all the ions that are produced due to thermal generation had been moved to the opposite electrodes and rate of generation and decrease due to outflow boundary condition is the same so we have no changes in ion concentration. Ions close to the electrodes before the application of the voltage are in equilibrium with the free ions in the bulk of liquid far away from the electrodes and their concentrations result from Boltzmann distribution [6].

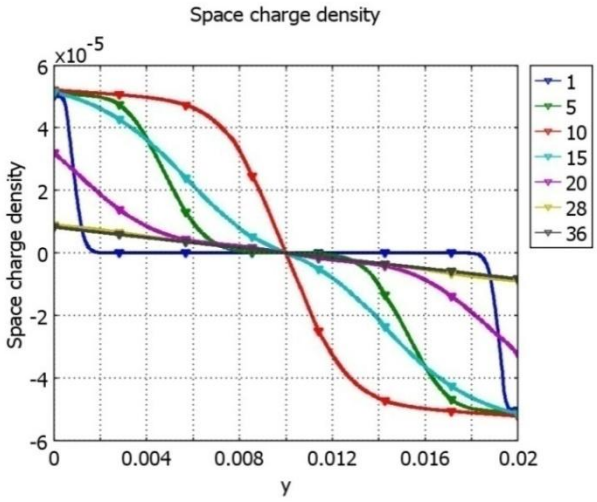

Figure 7. Time variation of the space charge density [c/m^3]

Time variations of space charge density shown in Figure 7; where formation of heterocharge (the charge with opposite sign of the electrodes) and evolution of charge at boundary layers can be seen. The experiment result of simple uniform field oil gaps shows that heterocharge accumulates near the electrodes [8]. Low value of space charge density is due to low conductivity of the oil. The formation of heterocharge near to the electrodes lead to a minorincrease of the electric field in those regions as it can be seen in Figure 8.

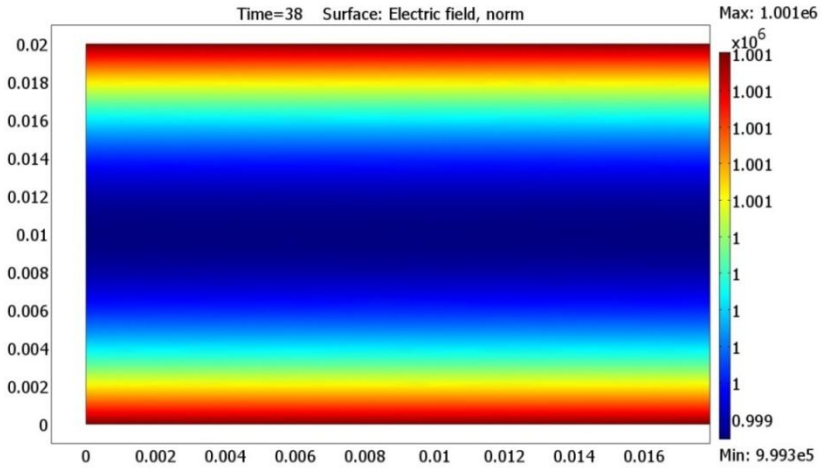

Figure 8. Electric field norm, steady state

Physical model and accurate measurement of electric field distribution is of interest for designing converter transformer. As it can be seen in Figure 9, the variation of electric field normal is not much. The reason is that the magnitude of space charge density is not high enough to produce strong distortion of the initial field. The highest distortion from the initial electric field value appears after 10s, where space charge density has the maximum value at different point in the bulk of oil.

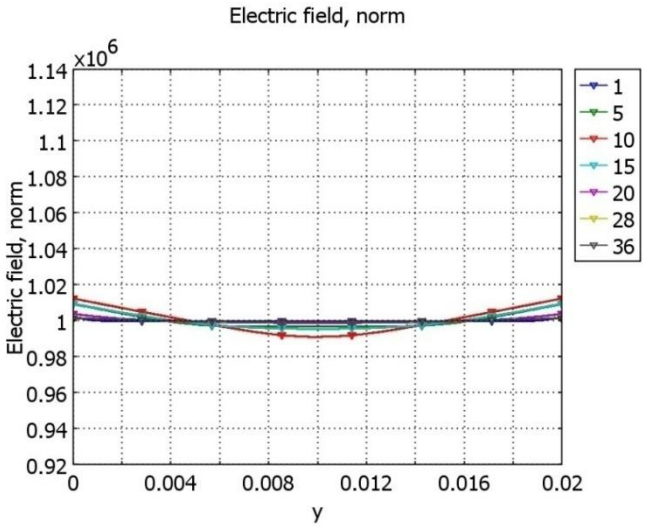

Figure 9. Time variation of electric field in oil gap

If the electric field distribution over a gap from the experiment and a simulation match together while injected concentration are put to zero in boundary condition then one can say that type of oil does not accept considerable amount of injected charge carriers from the electrode [8].

The electric field distribution in the gap can be predicted by the quotient of the transit time of an ion through the gap $\tau_{transit}$ and relaxation time τ_{relax} :

$$\kappa = \frac{\tau_{transit}}{\tau_{relax}} = \frac{\frac{d}{\mu V/d}}{\frac{\varepsilon_0\ \varepsilon_r}{\sigma}} \tag{37}$$

For $\kappa \ll 1$ ions sweep out of the gap before their relaxation leads to a uniform electric field distribution. For $\kappa \gg 1$ the relaxation time is faster than the transport time so the field will be increased near to the electrodes. However asymmetries in the electric field developed in a longer gap with higher voltage application, which cannot be predicted by simple charge separation heterocharge picture [8].

Hetero-charge accumulation on electrodes surfaces leads to field amplification at the electrodes which in the experiment can be due to the dissociation (of pollution) in bulk as the main source of charge carriers. If instead injection of charge carriers had been dominant contribution, charges of the same sign of the electrode result in a reduction of the field at the injecting electrode. The injection is visible especially in a case that $\kappa \ll 1$ [29].

$$\kappa = \frac{d^2}{\varepsilon\varepsilon_0 \rho.\left(\mu_n + \mu_p\right).V} \tag{38}$$

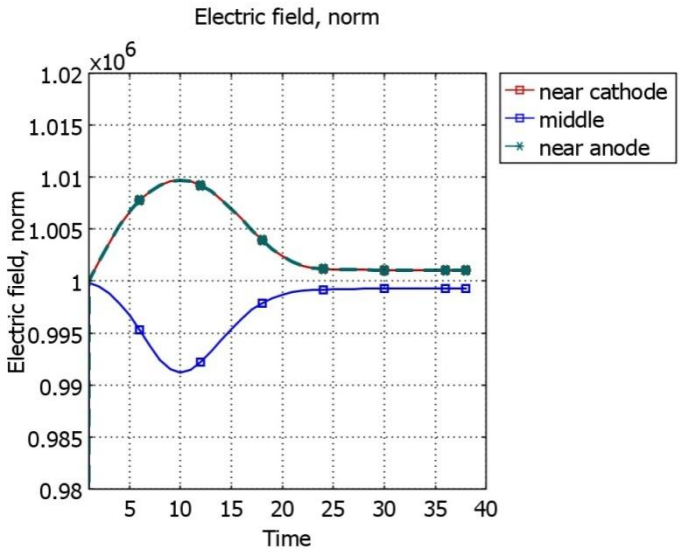

Figure 10. Electric field vs. time at three points

Normal electric field at three points (near cathode, middle of the bulk, near anode) can be seen in Figure 10. Beginning point of the curve is from time equal to 1s.
The ionic current curve is obtained by boundary integration of convective flux multiplied by elementary charge on the electrode surface with using Postprocessing → Boundary integration, Figure 11.

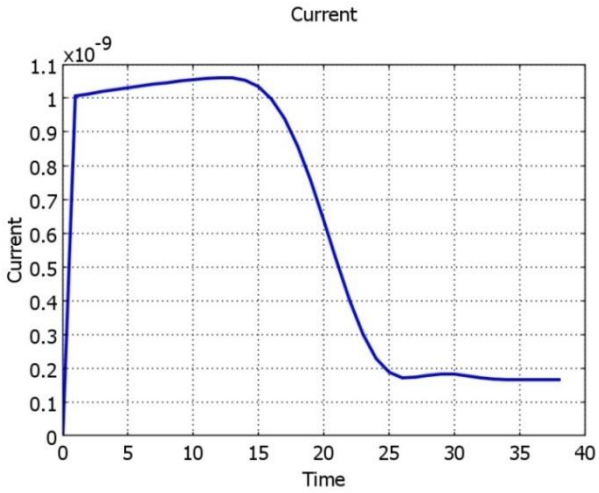

Figure 11. Ionic current

In a very simple picture it can be assumed that the layers of the ions are moving towards the opposite electrode which gives a constant current. When all the ions reach to the opposite electrode the current suddenly decrease to its steady state value, In a step-like manner. However in reality the current is going up and decreasing with a certain slope. Up to the first second the applied voltage increases to its maximum value. From 1s to around 15s the ions are moving towards the opposite electrode. The current has a small increasing tendency during this period because of the increase in ions concentration at electrode surface, which leads to higher electric field at this period. The time needed for the current to reach the maximum value is depending on the applied voltage, gap distance and ion mobility. Integration on the cathode or anode will give the same result since it is a symmetric case.

After 15s the current is decreasing and it is the start of sweep out process. If the current has a sharp decreasing slope then obtaining the transit time of the ions to the opposite electrode will be easy and precise.

In the simple model with neglecting the charge recombination, space charge effects and the bulk liquid motion the ion drift current should be constant until the ions are reaching to the opposite electrode and then decrease. From the current versus time curve the charge carrier mobility can be calculated [29].

The steady state value of the ionic current, $\mathrm{I_{ss}} = \int \mathrm{source_{ss}}$, is $0.18 \times 10^{-9} A$ and it is not zero due to the fact there is always generation of ions in the bulk of the oil. In steady state $\frac{\mathrm{dn}}{\mathrm{dt}} = \frac{\mathrm{dp}}{\mathrm{dt}} = \frac{\mathrm{dQ}}{\mathrm{dt}} = 0$ and there is no change in ion concentration in time. Source term is: $\mathrm{Q} = \int \mathrm{e}(\mathrm{p} - \mathrm{n})\mathrm{dv} = \mathrm{P} - \mathrm{N}$. At the steady state the generation rate of the current is the same as the rate of the charges going out from the system.

In the formula for calculating of the conduction current density the diffusion term is neglected and just ionic drift term considered since diffusion flux is much less than the convective flux as it can be seen in the Figure 12 for a point in the middle of the bulk of the oil. In other words this problem is strongly convection dominated problem.

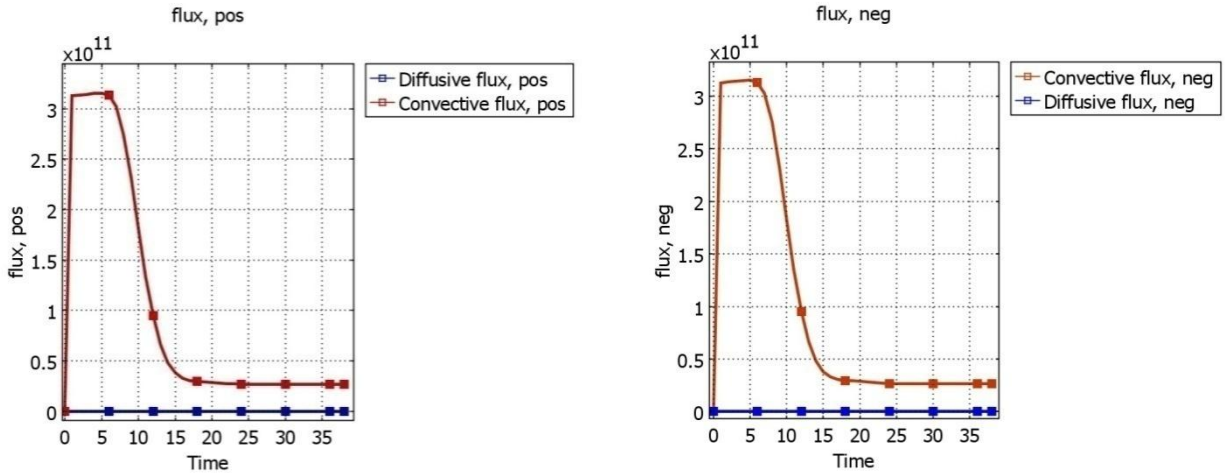

Figure 12. Convective and diffusive flux for positive and negative ions

Displacement current is defined by the rate of change of the field:

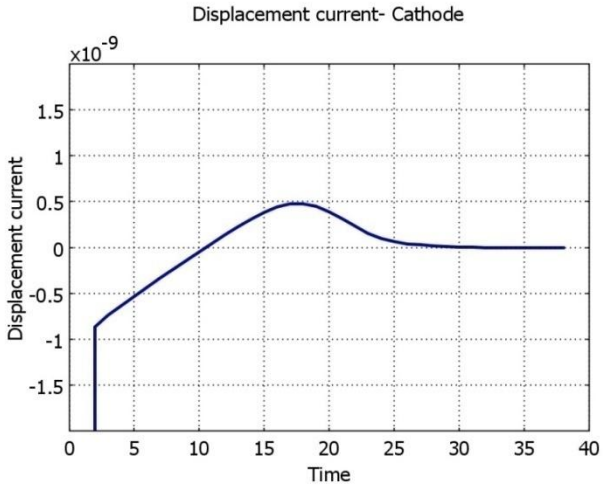

Figure 13. Displacement current at the cathode

By applying a voltage, displacement current can be measured while ions not reach the opposite electrode. At steady state displacement current is zero since no changes of electric field take place and even if charge movement is present, but when one charge is moves forward the other one takes its place. It is possible to compensate the displacement current due to voltage ramp but not for the ion movement.

Total current can be calculated on the electrode surface from the Maxwell's equations. It is a sum of injection current from the electrodes, conduction current which is proportional to the number of ions actually discharged per unit time per unit length of the electrode and the displacement current due to the permittivity ε like capacitor which is basically the surface charge change per unit length per unit time [23].

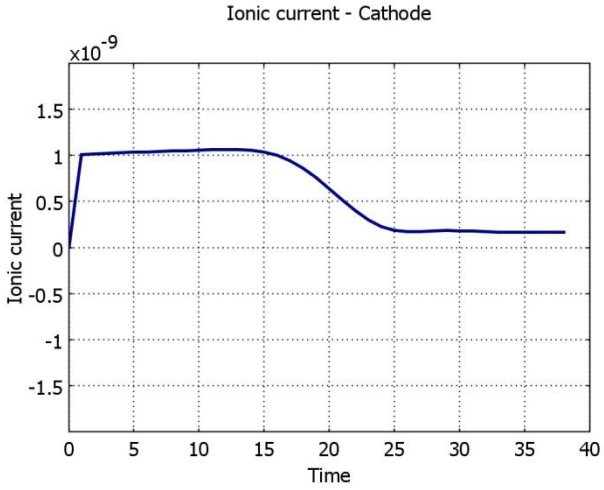

Figure 14. Ionic current at the cathode

Total current in Figure 15, is the sum of ionic current and displacement current since the injection current is neglected in this case. Integral of the source term in the bulk is equal to the total charge generation $\frac{dQ}{dt}$ in the bulk.

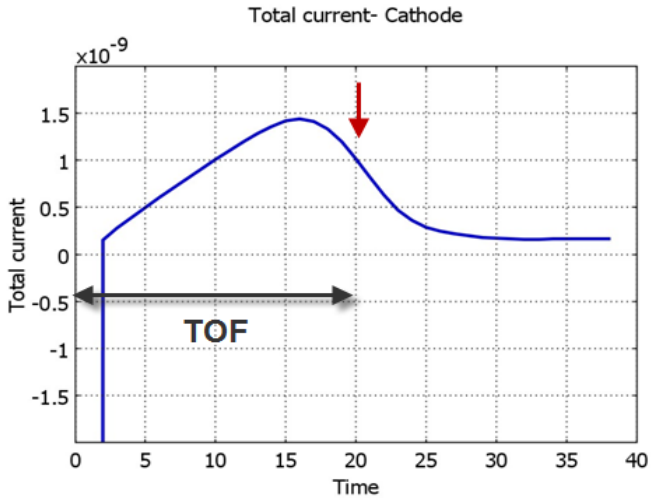

Figure 15. Total current at the cathode

As explained in section 2.3, the mobility of the ions can be calculated by knowing the time of flight (TOF) of ions according to formula (28). The mobility of the ions for case A is:

$$\mu = \frac{d^2}{Vs} = \frac{(20 \times 10^{-3})^2}{20 \times 10^3 \times 20} = 1 \times 10^{-9} \frac{m^2}{Vs}$$

Which is equal to the mobility of the ions used as a input of the simulation. The transit time of the ions can be selected between the initial rise of the current and the inflection point of the decay on the current vs. time curve. It is also possible to select the time between the initial rise of the current and the point where it falls to the one-half of the steady state current.
A simulation for 10 kV voltage with the same other conditions give almost the same result and showed that by decreasing the applied voltage we observe:

- Longer time, around 55 second, needed to reach the steady state.
- Higher value of ion concentration on electrode which leads to higher value of final steady state space charge density on the electrodes surface. The steady state value of the concentration is higher comparing to 20kV case because it takes longer time to reach steady state which means more generation of new ions in longer period of the time. Higher value of space charge density leads to larger distortion of normal electric field distribution from the initial value.
- Time variation of the current is similar to the previous case while lower electric field gives lower amplitude of current and also the fly time is almost doubled.

3.1.1.1 Mobility change, $\mu_- = \mu_+ = 3e^{-9}\ \frac{m^2}{Vs}$

The effect of changing the mobility value was investigated for the case A - low conductive oil.

The model and all the conditions are similar to those described in previous section 3.1.1 but the value of positive and negative mobility is changed to $3e^{-9}\ \frac{m^2}{Vs}$.

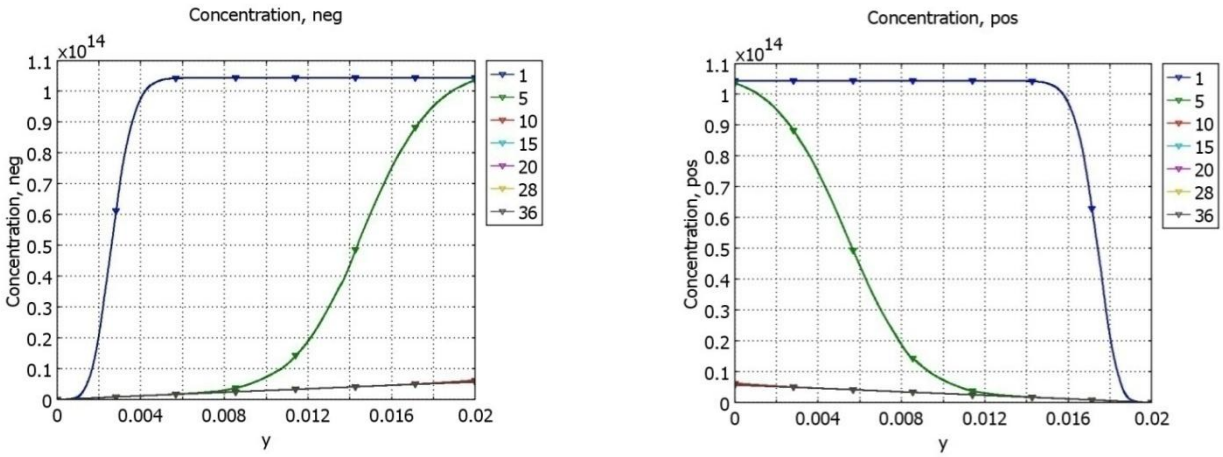

Figure 16. Time variation of ion concentration mobility $\mathbf{3e^{-9}\ \frac{m^2}{Vs}}$

It can be seen that increasing the mobility to $3\mathrm{e}^{-9}\ \frac{\mathrm{m}^2}{\mathrm{Vs}}$ leads to higher drift velocity value which means less time is needed for reaching to steady state condition. In this case steady state is reached almost at 10 second. Equilibrium density of ion concentration is reduced compared to previous case since the mobility in the denominator is increased.
Space charge density has a lower steady state value since the steady state value of ion concentration had been decreased.

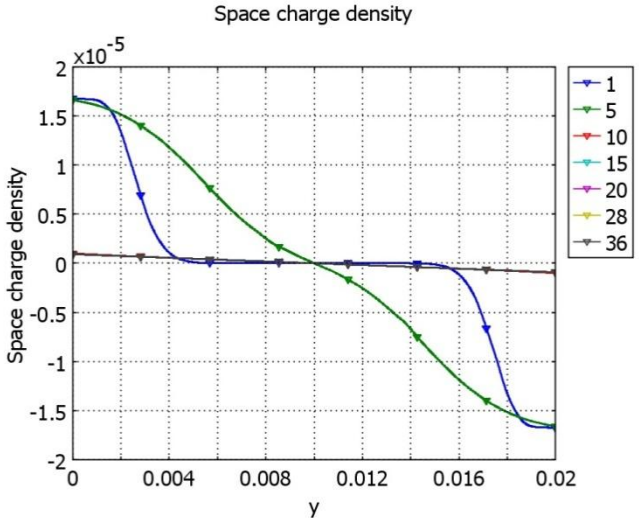

Figure 17. Time variation of the space charge density- mobility $\mathbf{3e^{-9}\ \frac{m^2}{Vs}}$

The equilibrium and steady state value of ion concentration and consequently space charge density can remain unchanged if the equilibrium density of charge carriers (n_0), formula 7, remains constant while the value of mobility had been changed. To do this, the conductivity should be multiplied by 3. Increasing the conductivity is the cause of increasing the amplitude of the current.

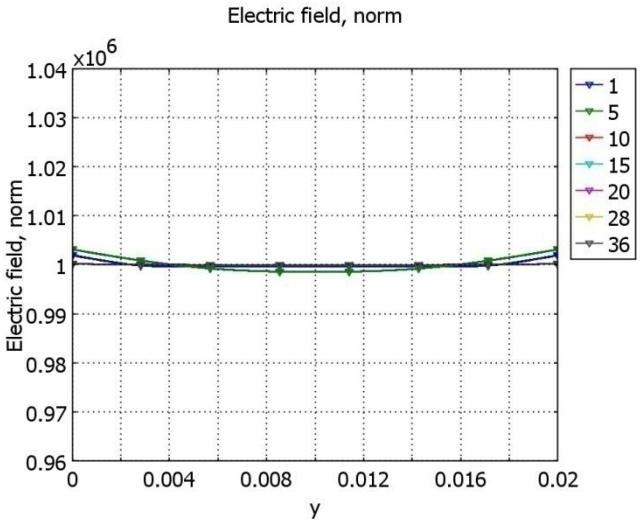

Figure 18. Time variation of electric field in oil gap- mobility $3\mathrm{e}^{-9}\ \frac{\mathrm{m}^2}{\mathrm{Vs}}$

Time variation of electric field can be seen in Figure 18, which shows a lower distortion from initial value due to lower space charge density.

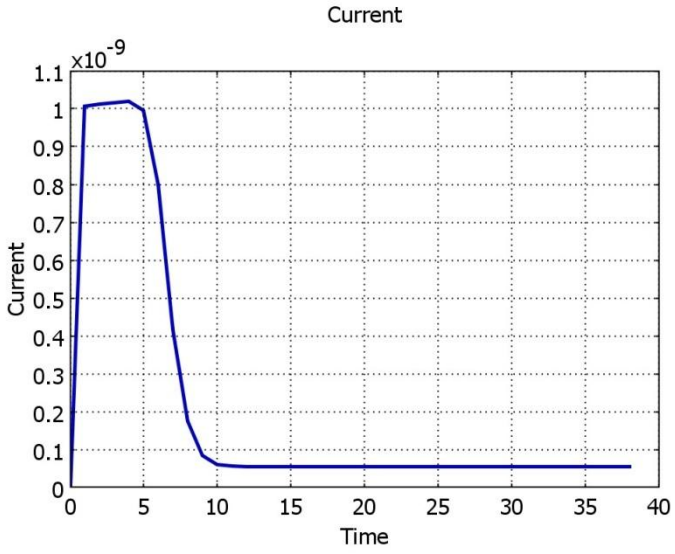

Figure 19. Ionic current at cathode mobility $3\mathrm{e}^{-9}\ \frac{\mathrm{m}^2}{\mathrm{Vs}}$

The current curve is similar as in the previous case with two differences: first it reaches the steady state value much faster and second the final value of the steady state current decreased since the steady state ion concentration decreased considering higher ion mobility and outflow boundary condition at the electrode surface comparing to the case with $1\mathrm{e}^{-9}\ \frac{\mathrm{m}^2}{\mathrm{Vs}}$ mobility.

3.1.1.2 Unsymmetrical mobility, $\mu_- = 3e^{-9}\ \frac{m^2}{Vs}$, $\mu_+ = 1e^{-9}\ \frac{m^2}{Vs}$

The model and all the conditions are similar to those used in previous section 3.1.1, the only difference is that the value of negative ion mobility is changed to $3e^{-9}\ \frac{m^2}{Vs}$ while the positive ion mobility remains unchanged ($1e^{-9}\ \frac{m^2}{Vs}$).
Concentration of positive ions is similar to the case 3.1.1 and concentration of negative ion is similar to the previous case.

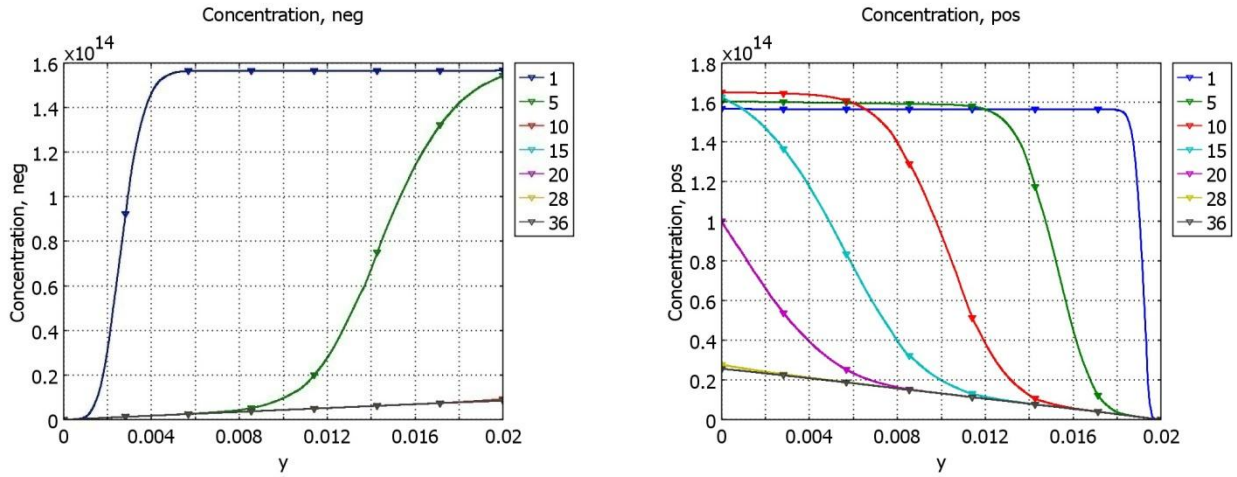

Figure 20. Time variation of the ions concentration- negative mobility $3e^{-9}\ \frac{m^2}{Vs}$

Space charge density is not balanced in the bulk and at electrode surface anymore, which leads to unbalanced electric field distribution. The charge carrier with the lower mobility contributes most to the space charge [29].

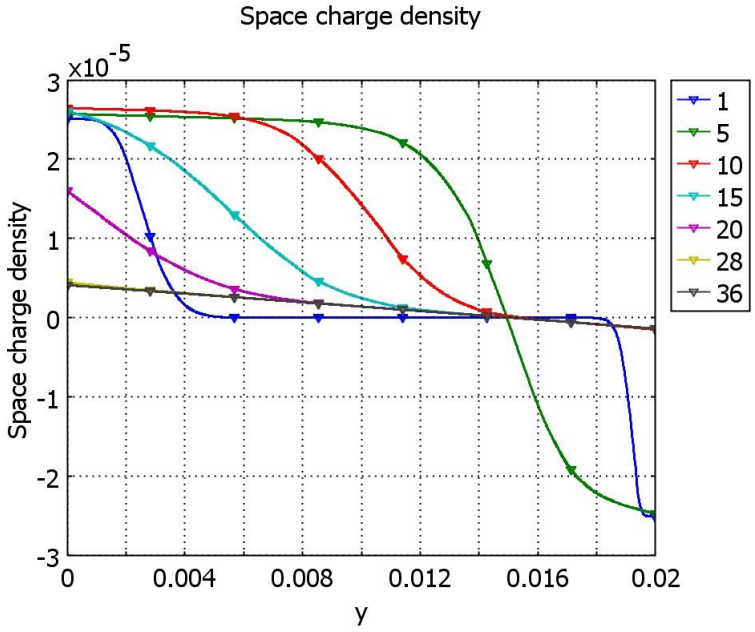

Figure 21. Time variation of the space charge density- negative mobility $3e^{-9}\ \frac{m^2}{Vs}$

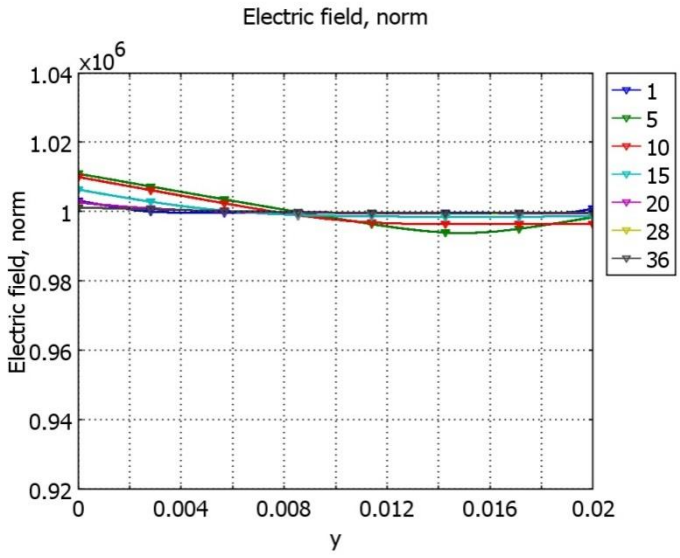

Figure 22. Time variation of electric field in oil gap- negative mobility 3e^{-9} $\frac{m^2}{Vs}$

By applying different mobilities of charge carriers for positive and negative ions the field curve becomes asymmetric. Distortion of the electric field near to cathode is higher as compare to near to anode because of higher concentration of positive ions.

The previous studies [27], showed that the asymmetry of the electric field distribution in the gap observed in the steady state is mainly due to the different mobilities of the two types of charge carriers and not due to the injection from a electrode.

Therefore if the asymmetry in the electric field distribution depends on the polarity then it suggests for existence of different mobilities of the positive and negative ions rather than injection of charges at the electrodes [1]. Though in general, existence of asymmetries in the field distribution in bulk of the oil may not only be due to different mobilities of positive and negative ions but also injection from the electrodes.

The ionic current curve at the cathode and anode is given in Figure 23.

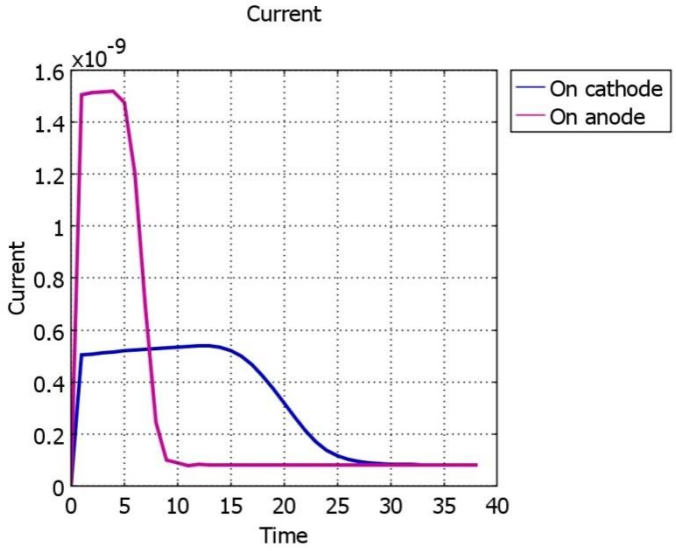

Figure 23. Ionic current at cathode / anode - neg mobility 3e^{-9} $\frac{m^2}{Vs}$

3.1.1.3 Resistivity change

The effect of increasing and decreasing the resistivity on the current curves is studied in this section. The parameter of the simulation is as follow:

Negative ion mobility is equal to the positive ion mobility, i.e. = $1e^{-9}\ \frac{m^2}{Vs}$. Gap distance is=10mm, voltage is=10kV and no injection. The current curves scaled with a scaling factor= 0.395, which is calculated by considering the electrode diameter of 100 mm in a test set-up. The artificial diffusion, maximum mesh size in the bulk and rise time of the applied voltage are equal to the parameters obtained after parameter sensivity tests, Appendix B.

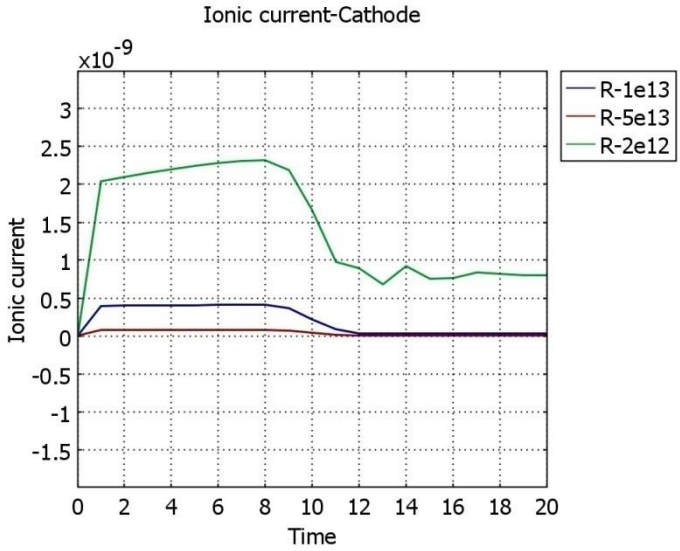

Figure 24. Ionic current at cathode

As it can be seen in Figure 24; by decreasing the resistivity the current amplitude increases and vice versa. Decreasing the resistivity will leads to oscillation before steady state current is reached due to the numerical issues.

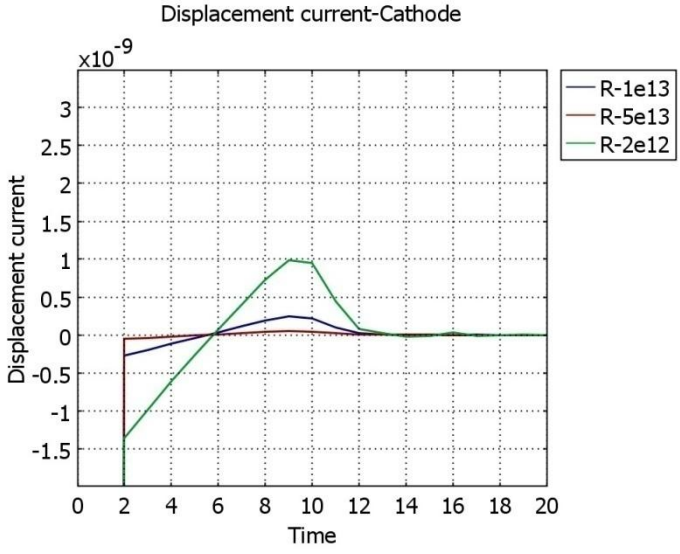

Figure 25. Displacement current at cathode

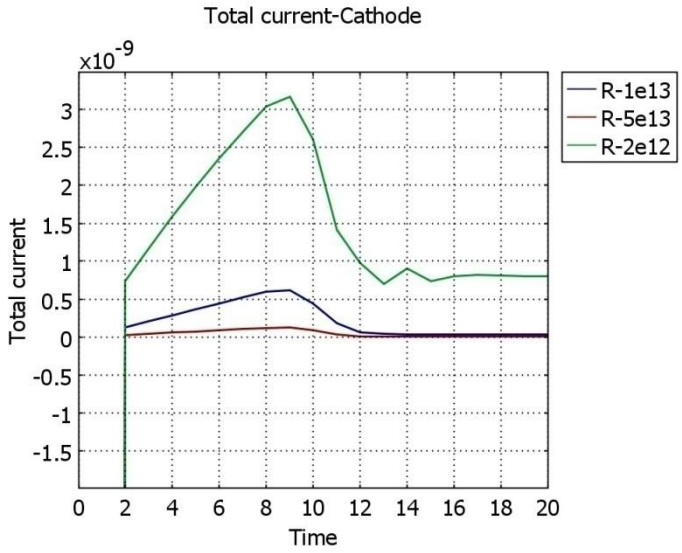

.

Figure 26. Total current

A model based on charge carrier generation by dissociation of ion pairs in the bulk of the liquid describes the electric field distribution well in high resistive oil but this approach fails when increasing the liquid conductivity [27].

3.1.2 Case B – Low conductive oil, σ = 10-13 S/m, negative ion injection from cathode

In the following part the injection of negative ions is implemented in COMSOL file by selecting flux boundary condition for cathode and anode. The mobility of positive and negative ions is 10^{-9} [m^2/Vs]. The reason for selecting negative ion injection is that in transformer oil negative ion injection is the dominant injection type [5].The injection is described by Eq. (25) and (26).
It can be seen in Figure 27 that concentrations of positive ions have the same time variation as the case 3.2.1, while negative ion injection on cathode is the reason for higher steady state negative ion concentration.

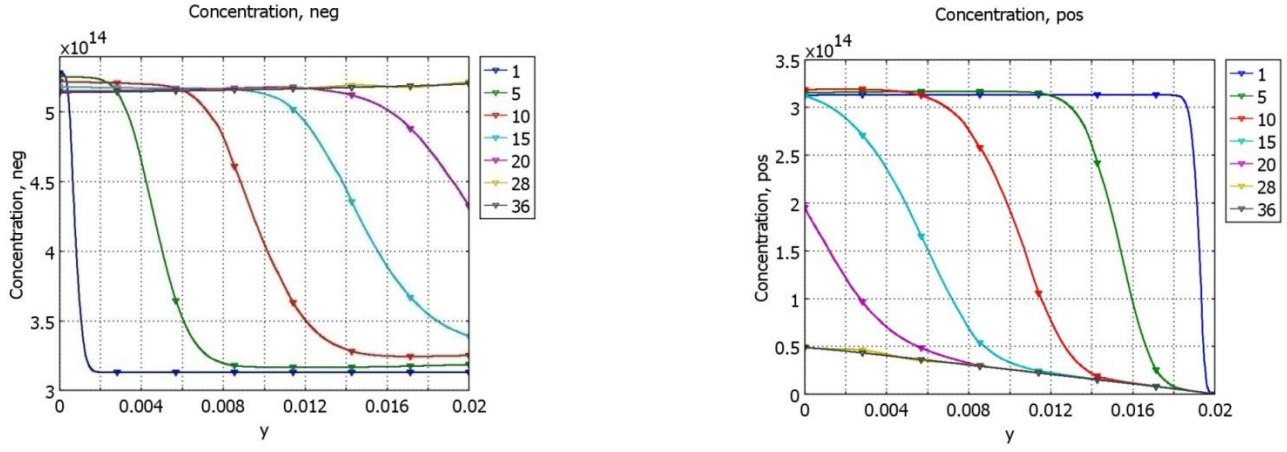

Figure 27. Time variation of the ions concentration

Figure 28 shows that both cathode and anode are negatively charged and heterocharge dominated regime in a case without injection changes to homocharge dominated system. The middle of the gap is not neutral any more. The time needed to reach the steady state is 30 second, the same as without injection.

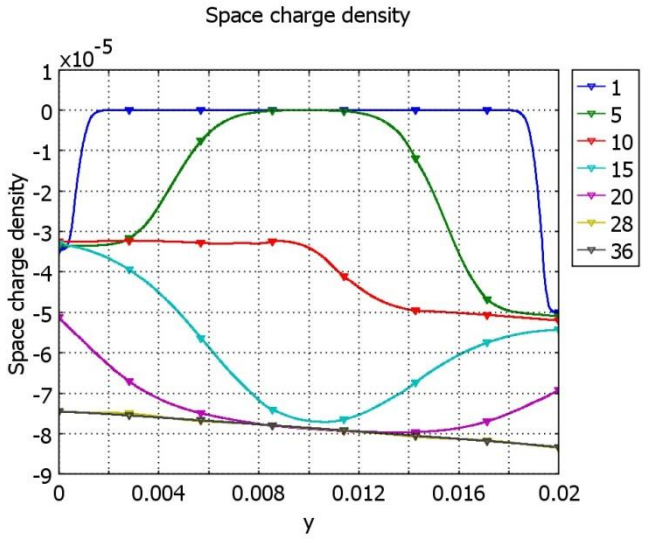

Figure 28. Time variation of the space charge density

The amounts of the charges in the gap, which are generated in the bulk of oil or injected from the electrodes, depend on the equilibrium concentration of the ions and it is low for low conductive oil. The higher volume of oil has no effect in the ion injection on the electrode surface. Higher volume the more ions are generated in the bulk of the oil.

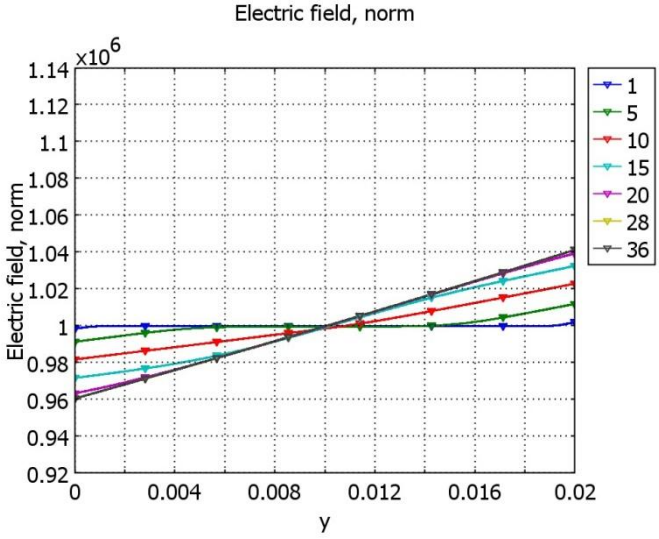

Figure 29. Time variation of electric field in oil gap

Electric field distortion from the initial value, Figure 29, is higher than in the case without injection but still it is not too much large since numbers of charges are low in the low conductive oil.

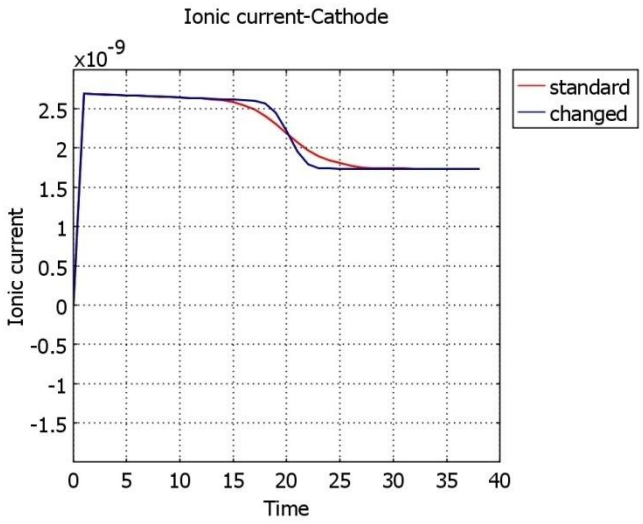

Figure 30. Ionic current – cathode

As it can be seen from Figure 30 the current on cathode is similar to the previous cases with the differences that at the beginning the current has a decreasing slope which is due to the higher value of the convective flux of negative ions comparing to the value of convective flux of positive ions. It can also be explained by the fact that electric field is decreasing on the cathode surface because of higher concentration of negative ion on the cathode surface. After 15 seconds the effect of negative ions become dominant and current has a steeper decreasing slope and the steady state current is reached at around 27 seconds with the higher value comparing to the case 3.1.1 due to negative ion injection.

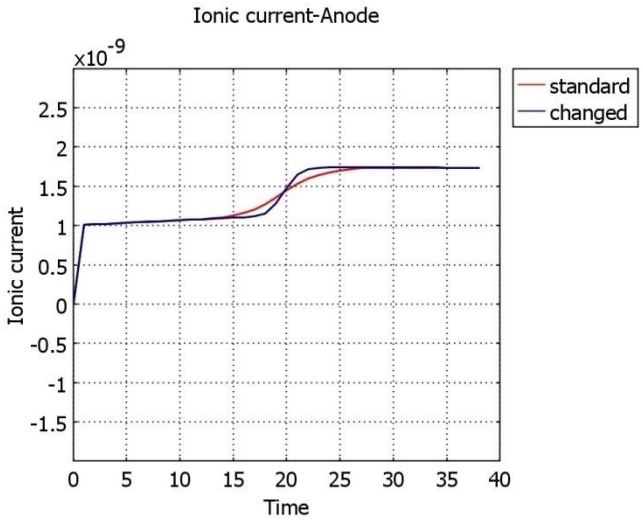

Figure 31. Ionic current – anode

The current at the anode during period of 1 s to 15 s is more due to ion generation in the bulk with a small increasing slope due to increasing of the electric field. The negative ion

injection causes the current increase from between 15 and 25 seconds. The steady state is reached after about 27 seconds when there is no more change in ion concentration and in the electric field distribution.

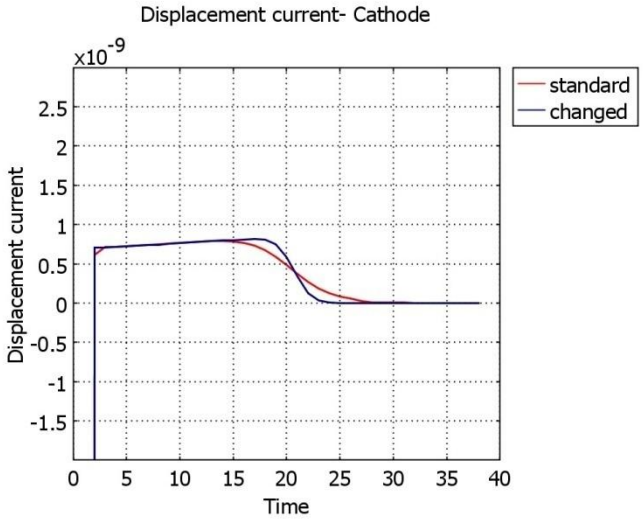

Figure 32. Displacement current- cathode

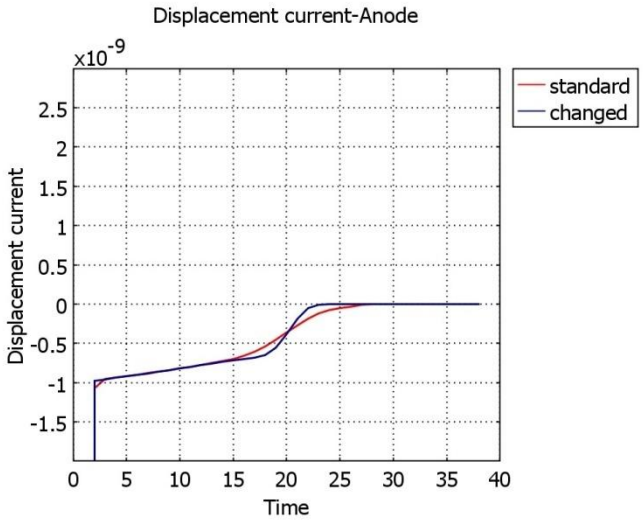

Figure 33. Displacement current - anode

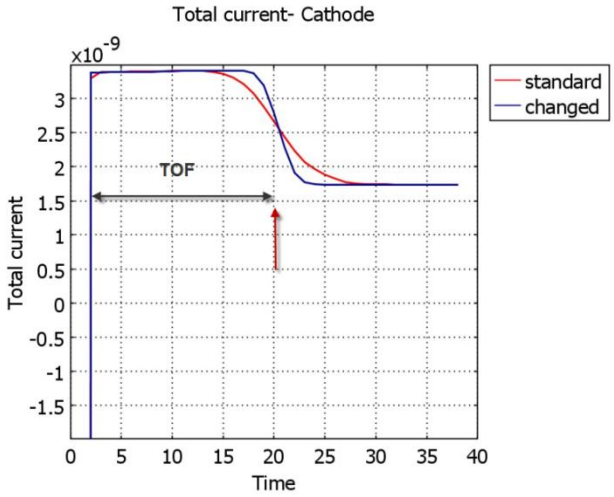

Figure 34. Total current- cathode

The mobility of the ions can be calculated by obtaining the time of flight from the current curve as illustrated in the Figure 34.

$$\mu = \frac{gap\ distance^2}{Voltagesecond} = \frac{(20 \times 10^{-3})^2}{20 \times 10^3 \times 20} = 10^{-9} \frac{m^2}{Vs}$$

The calculated mobility from the current curve is equal to the mobility have been used as input for the simulation.

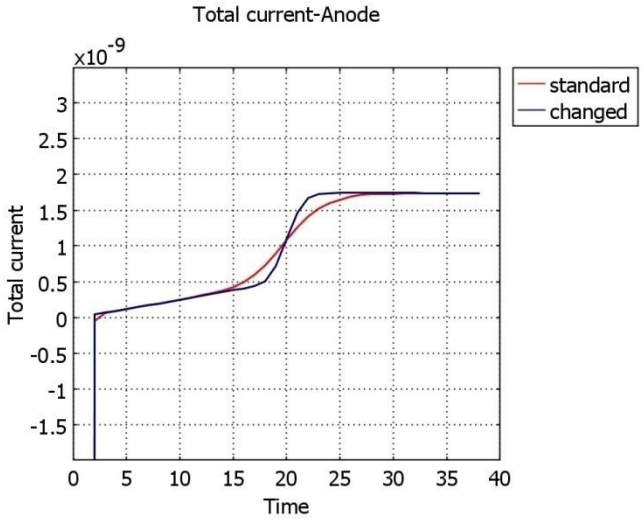

Figure 35. Total current- cathode

Note: In Figure 30 to Figure 35, the abbreviation “standard” refer to the non- modified and “changed” to the modified cases of the parameters in the simulation. More details of parameter optimization are given in Appendix B.

There are two reasons for increase of the current by applying the dc voltage: the field enhanced dissociation of weak electrolytes and the injection of charges on electrodes. Existence of ion injections was experimentally proved even in low applied fields (200 Vcm-1) in hydrocarbons [6].

In a summary the component of the total current in two time interval can be given as below:

I) $0 < t < t_{sweep\ out}$ $I_{tot} = I_{sweep\ out} + I_{Disp.} + I_{inj} + I_{source}$ (39)

II) $t > t_{\mathrm{sweep\ out}}$ $\mathrm{I_{tot}} = \mathrm{I_{inj}} + \mathrm{I_{source}}$ (40)

The sweep out current $I_{sweep\ out}$ is the current due to the ions move out from the bulk of the oil, which already existed in the oil before voltage application and source current is the current from the ions generated in the bulk of the oil. I_{inj} is the injected current from the electrode and $I_{Disp.}$ is the displacement current.

The current difference between maximum value and steady state of the current is from the sweep out current plus the displacement current. The current in steady state has two components: injection + source term.

4 EXPERIMENTAL

In this chapter the experimental set-up and schemes of data acquisition systems are illustrated. The result and discussion of the experiment follows thereafter.

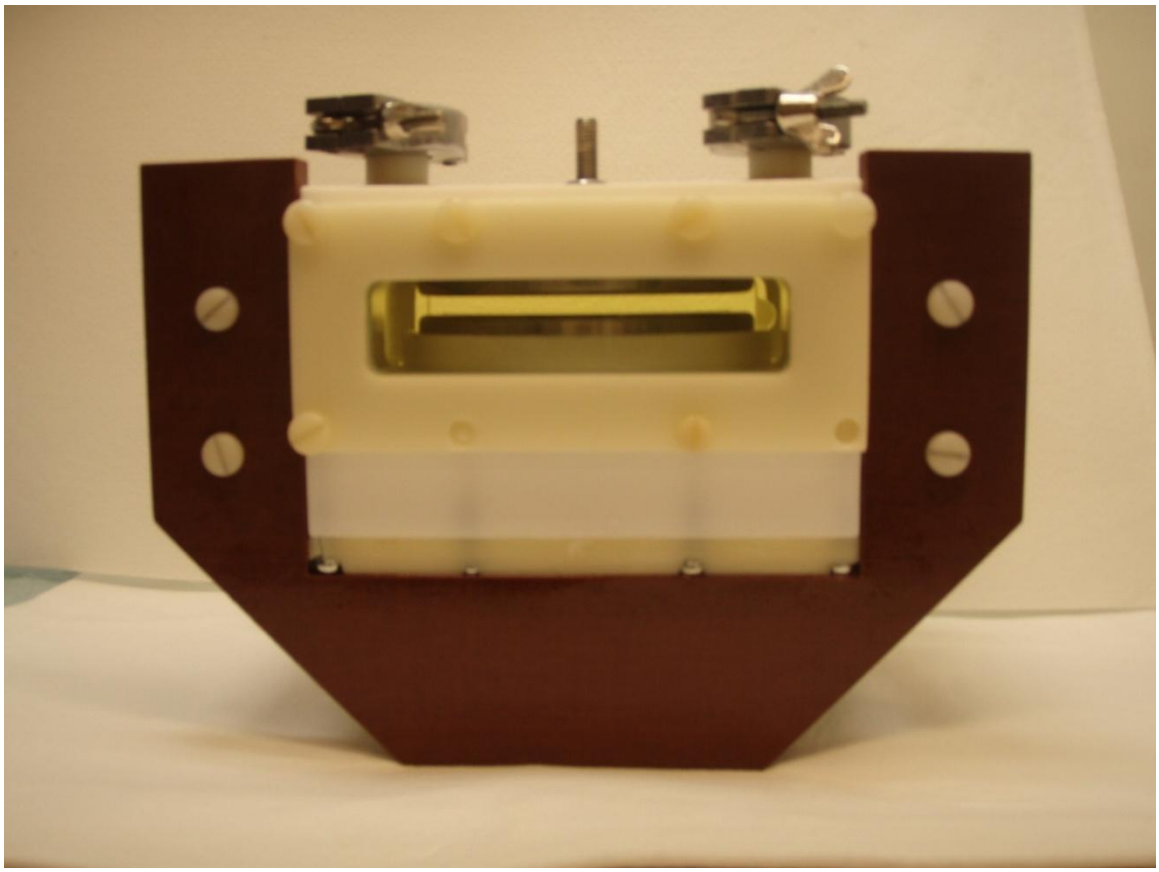

Figure 36. Test cell

4.1 Experimental set-up

The test set-up consists of measuring cell and data acquisition system. The Teflon® test cell, Figure 36, has a 300 ml oil capacity with two flat polished stainless steel electrodes of 100 mm diameter. At its top the cell has two pipes for filling it with oil and a connection to high voltage electrode. The current measuring electrode has a guard ring which is separated from collecting electrode of 84 mm diameter with insulation. The gap distance can be regulated up to 19 mm.

Different measurement systems were tested to find suitable test set-up. The method for measuring the ion mobility, as discussed in previous chapter, is by applying the voltage to the high voltage electrode to get the current signal. From the current signal the time of flight of the ions is obtained. The time of flight is the time the ions travel from one electrode to the opposite one. By knowing the gap distance, applied voltage and time of flight the mobility can be calculated according to formula (28).The first measurement system used is shown in Figure 37.

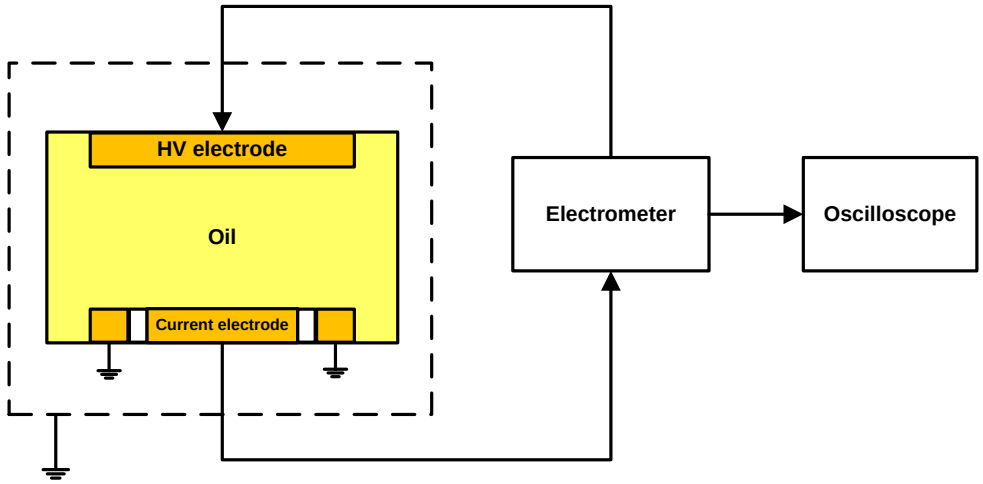

Figure 37. Set-up one

Set-up one is consisting of the test cell, electrometer and oscilloscope. In order to reduce the noise level on the output signal the test cell had been put into a grounded metallic bucket. The test cell was separated within a protective cage from the rest of the set-up for the security reason. By opening the door of the cage a relay turned off the voltage source.

The electrometer operates as both a voltage source and ampere meter with a digital display. Current curve can be seen in oscilloscope by BNC cable connection. This set-up helped to check the cable connection between cell and the electrometer. The problem of this set-up was that it was not convenient for saving the measured data in a computer.
In order to save the data in a computer a GPIB (General Purpose Interface Bus) had been used in set-up number two, Figure 38.

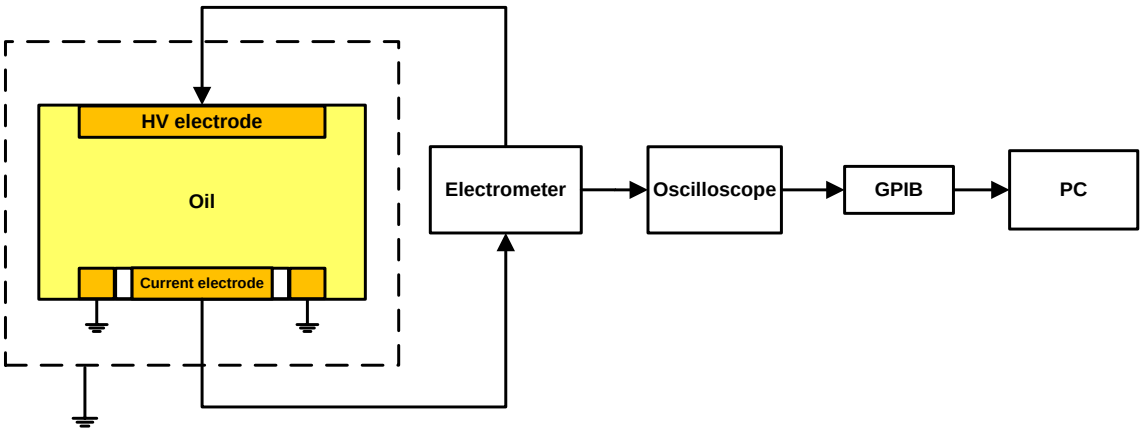

Figure 38. Set-up two

The software used for communication between GPIB and PC was “Manyscope” which had been developed at ABB Corporate Research. This configuration had a limitation on the time interval that it can store data of the output signal. Noise on the current signal is another problem of this set-up although the test cell was located in a metal bucket for shielding purpose.
The next step in improvement of the test circuit is to use a signal acquisition card connected to channel 1 of the oscilloscope via a T-connector, Data acquisition card gives the possibility to save the data for a longer time in a text format by using LabVIEW software. The signal on PC is the same as signal in oscilloscope.

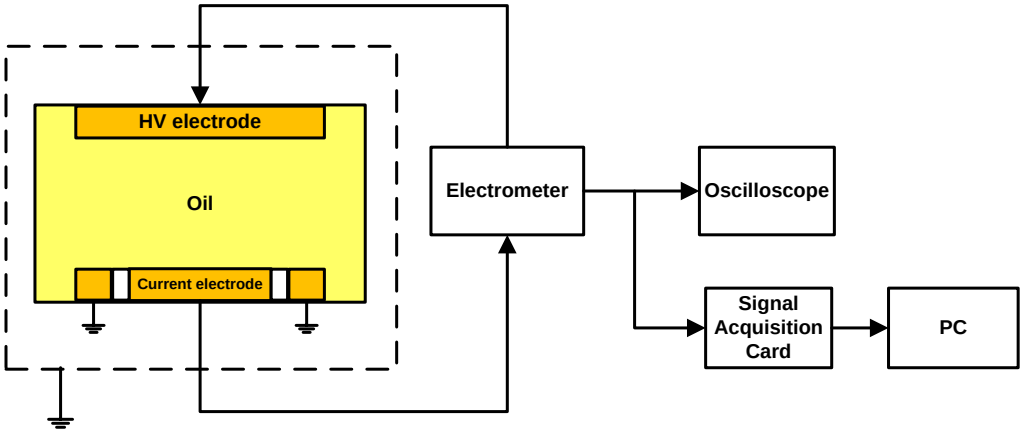

Figure 39. Set-up three

The oscilloscope measures voltage over a time so in order to convert saved data from a voltage to a current; one should know the current range set on the electrometer. Maximum output of the Electrometer is 2 V so for example: if 2nA range for current measurement is selected the voltage signal can be converted to current signal by following formula:

$$\text{Current on the Oscilloscope} = \frac{\text{Voltage on Osciloscope} \times 2\ \text{nA}}{2\ \text{V}} \qquad (41)$$

Decreasing the noise level is crucial for low voltage application. Further investigation showed that the noise level increased while the current signal was transferred from electrometer to the oscilloscope or data acquisition card. This tells that the noise level decreases significantly if data are collected directly from the electrometer. To do this, data were collected from the electrometer via GPIB by utilizing LabVIEW software, Figure 40.

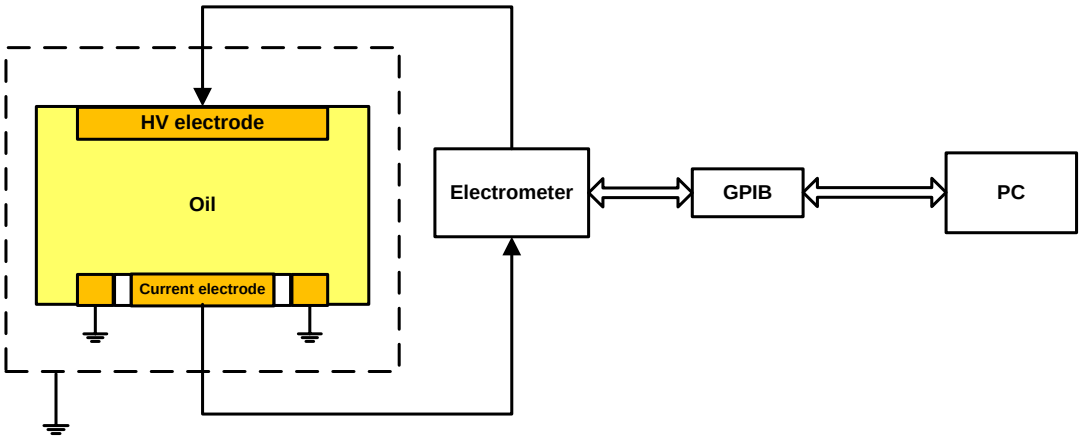

Figure 40. Set-up four

The picture of the test set-up in the lab can be seen in a Figure 41. In the left side of the picture the test cell is located in the bucket. The cage and the bucket are grounded. On the right side of the cage the electrometer can be seen. On the right side of the picture an oscilloscope is placed.

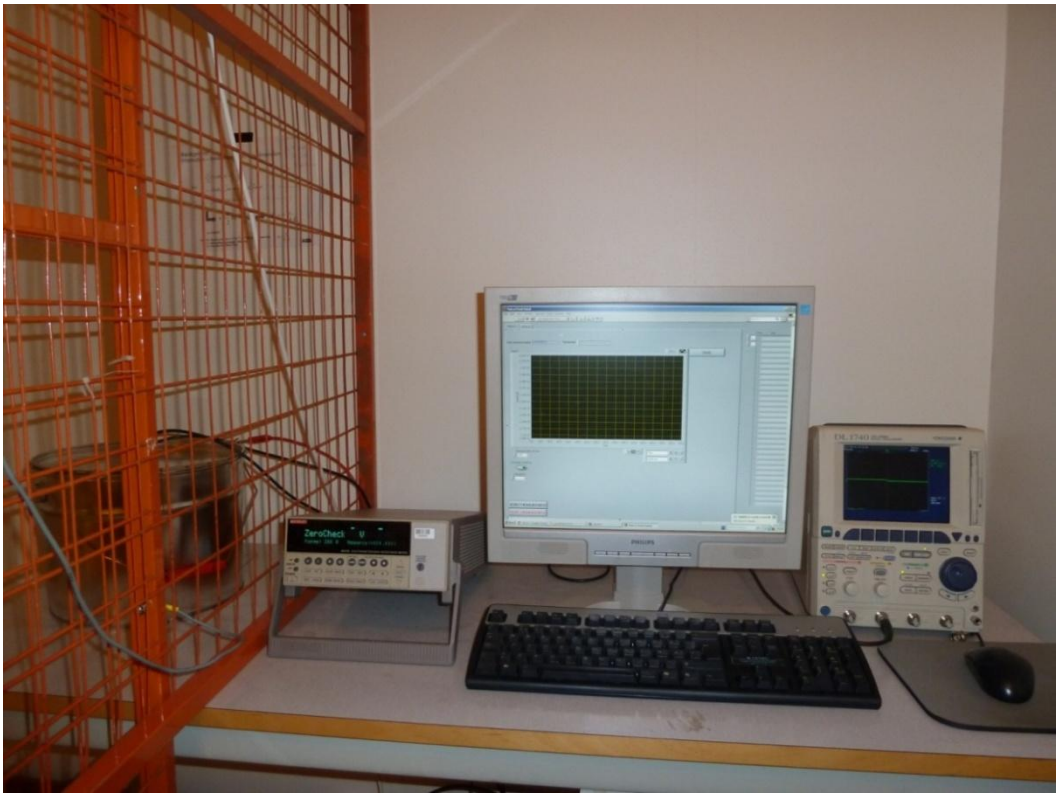

Figure 41. Test set-up in the Lab

4.1.1 Measuring instruments

The hardware used in the test set-up is listed in Table 1.

Table 1. Measuring instruments

Type	Model	Manufacturer
Oscilloscope	DL 1740	YOKOGAWA
Electrometer	6517A	KEITHLEY
Signal acquisition card	NI USB-6251	National Instruments
GPIB	GPIB-USB-B	National Instruments

4.1.2 Cleaning procedure of test cell

In order to start cleaning the empty cell first it had to be de-assembled. The de- assembled test cell had been cleaned with a solvent several times and then dried. When the cell was dry it could be filled with transformer oil.

4.2 Ion mobility measurement

All the measurements have been done at room temperature. No extra purification of the transformer oil had been done. The time interval between two tests was more than the relaxation time, ($Relaxation\ time = \frac{\varepsilon_0 \varepsilon_r}{\sigma}$). The relaxation time for the mineral oil is around 25 minutes and for the natural ester oil is around 15 second.

4.2.1 Single polarity method

In this part the result of experiment for single polarity method are given. The positive or negative polarity was applied to the high voltage electrode. From the measured current the time of flight was obtained. In this study we have chosen to define the time of flight (TOF) equal to the time interval between voltage application and the time that the current reached a local maximum value. Positive ion mobility is calculated from positive voltage application and vice versa.

- **Mineral Oil**

Mineral transformer oils are complex mixtures of paraffinic, naphthenic and aromatic hydrocarbons.

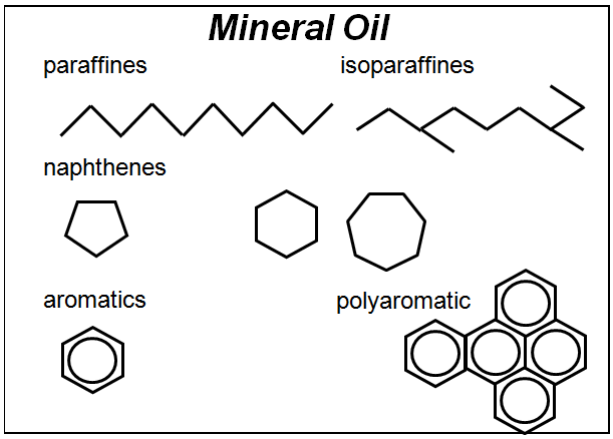

Figure 42. Mineral oil

The naphthenic oils that are less viscous and have good gas absorbing properties are more preferred over the other ones. The mineral oils have relative dielectric constant ε_r of around 2 and high resistivity which indicate low content of free ions [10].

The test cell was cleaned with ethanol and isopropanol before filling with the oil. Current curve for applying -1000 V to 5 mm gap can be seen in Figure 43. The mobility of the negative ions can be calculated from the test with negative polarity of the applied voltage.

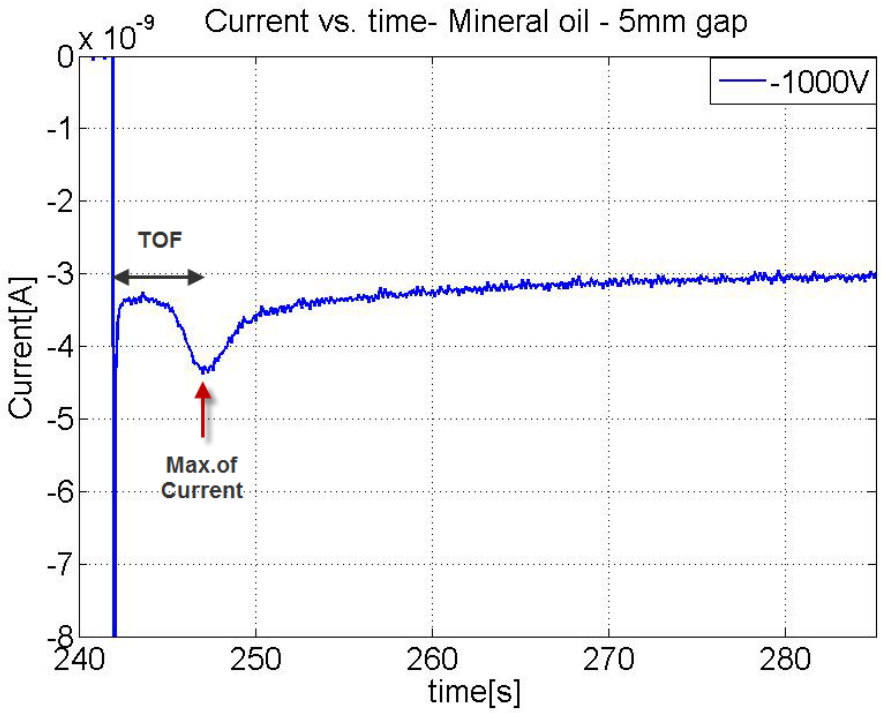

Figure 43. Current curve – Mineral oil – 5 mm gap

After one hour of applying -1000V the second test is done with +1000 V, Figure 44. From this experiment the mobility of the positive ions can be calculated by obtaining the time of flight. This experiment done with set-up three illustrated in Figure 39.

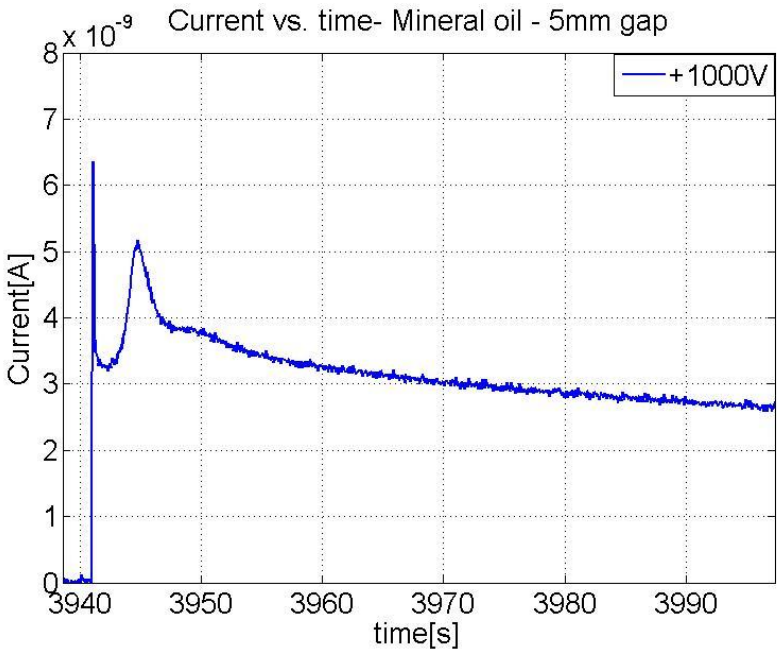

Figure 44. Current curve – Mineral oil – 5 mm gap

The table two shows the result for positive and negative voltage application:

Table 2. Mineral oil – 5 mm gap - set-up three

Oil type	Voltage	Gap	Electrometer range	Time of flight	Mobility[$\frac{m^2}{Vs}$]
Mineral oil	+1000 V	5mm	20 nA	4 sec	6.25 e^{-9}
Mineral oil	-1000 V	5mm	20 nA	5.2 sec	4.8 e^{-9}

It can be seen there is a difference between the current curves in simulation and experiment and the way to select time of flight for mobility calculation. The differences can be explained with help of a very simple picture of ion movement in the bulk of oil, Figure 45.

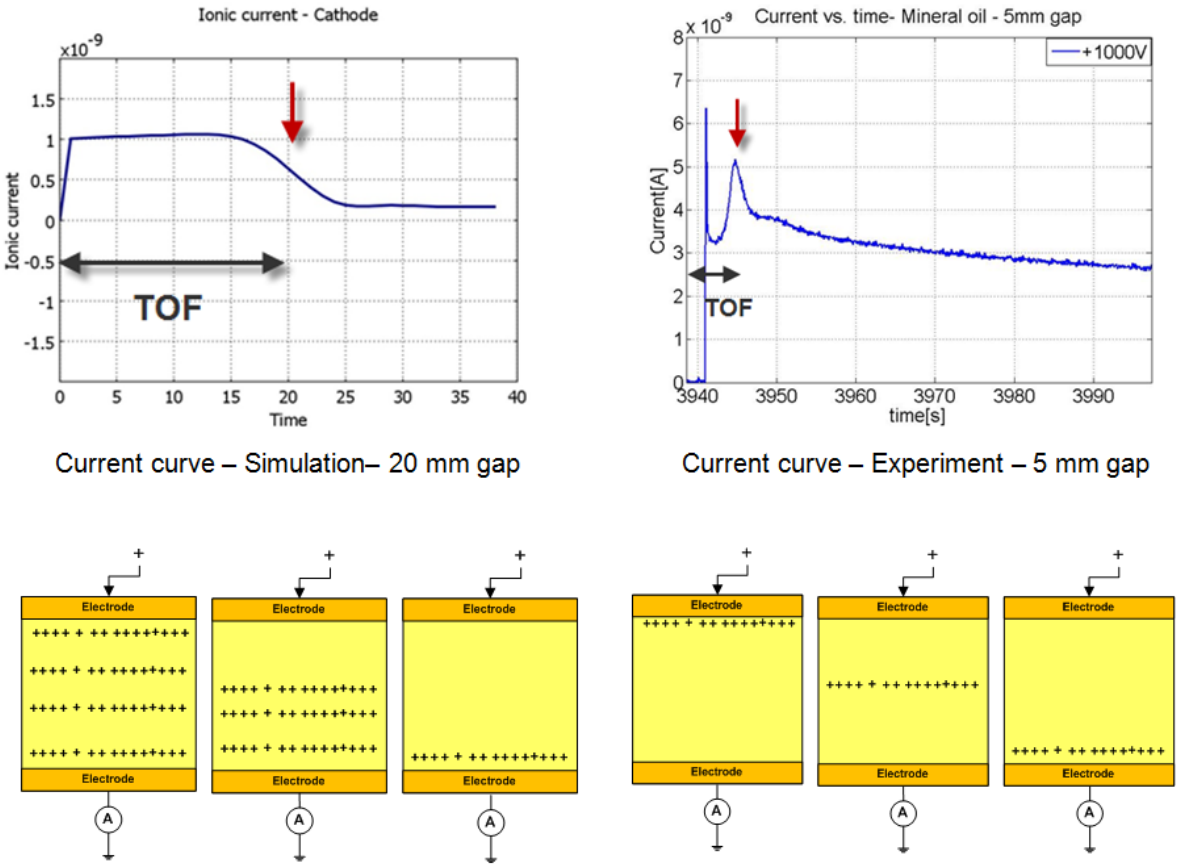

Figure 45. Mobility calculation – simulation vs. experiment

In simulation the current amplitude is almost constant up to the point the layers of ions are reaching to the collecting electrode and it start to decrease when the rate of ions in a time reaching to measuring electrode decreased. In experiment there is stored layer of ions on the electrode surface moving to opposite electrode by voltage application and when this layer of ions reached to collecting electrode it will gives the current peak.

The resistivity of the oil before test from the barrel was $8.78e^{13}$ [Ωm] at 0.01 Hz and the resistivity of the oil after test was $8.67e^{11}$ [Ωm] at 0.01 Hz. The dielectric relaxation time can be calculated as follows:

$$\tau_{relax} = \frac{\varepsilon_0\ \varepsilon_r}{\sigma} = \frac{8.854e^{-12} \times 2.2}{(\frac{1}{8.781e^{13}[\Omega m]})} = 1.71e^{3}\ \text{sec}$$

- **Natural Ester Oil**

Prior to the measurement, the test cell is cleaned with cyklohexan. The cyklohexan used as a cleaning solvent for all the tests except the first one because it was more effective for cleaning the cell. After the cell was dry it was filled with natural ester oil for the next series of tests using test set-up three. The chemical structure of the natural ester oil is given in Figure 46.

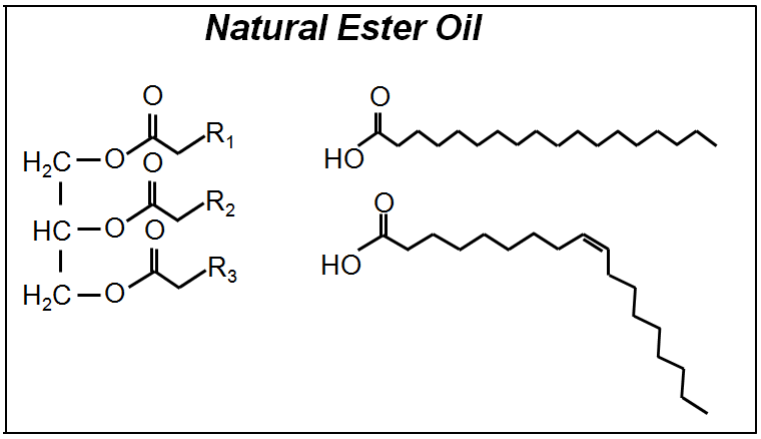

Figure 46. Natural ester Oil

The current curve of applying -1000V is given in Figure 47.

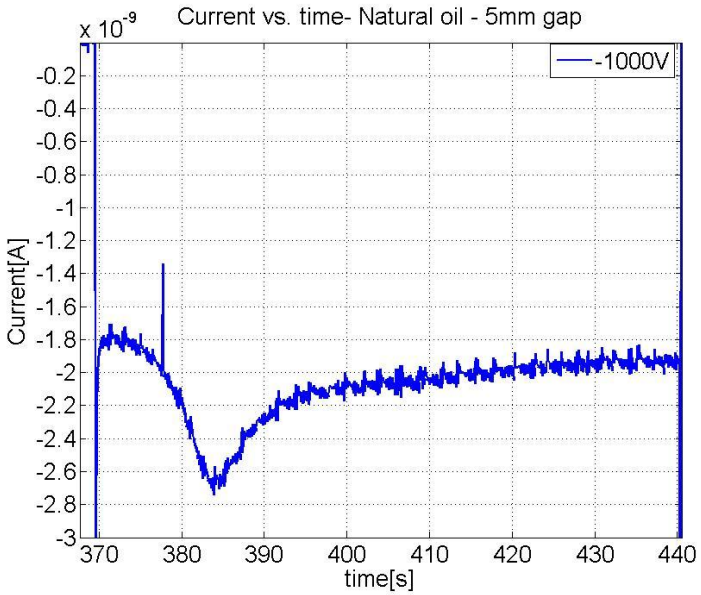

Figure 47. Current curve- Natural ester oil- 5mm gap

The next test had been done with +1000 V, Figure 48. The rest time was 74 minutes.

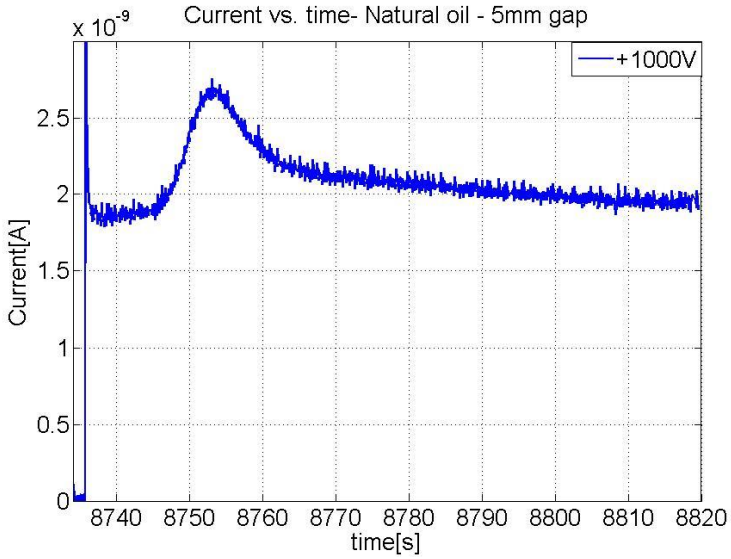

Figure 48. Current curve- Natural ester oil- 5mm gap

The table of result on natural ester oil for 5 mm gap distance obtained with test set-up three is given in Table 3.

Table 3. Natural ester oil – 5 mm gap - set-up three

Oil type	Voltage	gap	Electrometer range	Time of flight	Calculated Mobility[$\frac{m^2}{Vs}$]
Natural ester oil	-1000 V	5mm	20 nA	14.4 sec	1.74 e^{-9}
Natural ester oil	+1000 V	5mm	20 nA	17 sec	1.47 e^{-9}
Natural ester oil	+900 V	5mm	20 nA	22.5 sec	1.23 e^{-9}
Natural ester oil	-900 V	5mm	20 nA	17.88 sec	1.55 e^{-9}
Natural ester oil	-800 V	5mm	20 nA	27.5 sec	1.14 e^{-9}
Natural ester oil	+800 V	5mm	20 nA	21 sec	1.45 e^{-9}
Natural ester oil	+800 V	5mm	20 nA	34 sec	9.19 e^{-10}

The rest time between each test presented in Table 3 was more than one hour. The result of the test on the natural ester oil for a 5 mm gap with test set-up four is given in Table 4. The test procedure was applying the voltage to the high voltage electrode and then measuring the current.

Table 4. Natural ester oil – 5 mm gap – set-up four

Oil type	Voltage	gap	Electrometer range	Time of flight	Calculated Mobility[$\frac{m^2}{Vs}$]
Natural ester oil	+600 V	5mm	2 nA	38.75 sec	1.07 e^{-9}
Natural ester oil	+700 V	5mm	20 nA	31.75 sec	1.12 e^{-9}
Natural ester oil	+800 V	5mm	20 nA	26.25 sec	1.19 e^{-9}
Natural ester oil	+900 V	5mm	20 nA	21 sec	1.32 e^{-9}
Natural ester oil	+1000 V	5mm	20 nA	16 sec	1.56 e^{-9}

The dielectric relaxation time can be calculated as follow:

$$\tau_{relax} = \frac{\varepsilon_0\ \varepsilon_r}{\sigma} = \frac{8.854e^{-12} \times 3.12}{(\frac{1}{6.17e^{11}})} = 17\ \text{sec}$$

In this section the high voltage was selected for two reasons: first the noise level in test set-up three was high and decreasing the voltage level made impossible getting the desired output signal. The second reason was that the gap distance was 5 mm, thus low voltage led to low signal. In this pre experiment the application of high voltage caused el EHD movement in liquid and consequently the calculated mobility values were higher than the real ion mobility (apparent mobility) [19],[24]. In the next part the polarity reversal method was used in set-up four, providing a possibility to do the measurement in a lower voltage range and shorter gap distances, thus avoiding EHD oil movement.

4.2.2 Polarity reversal method

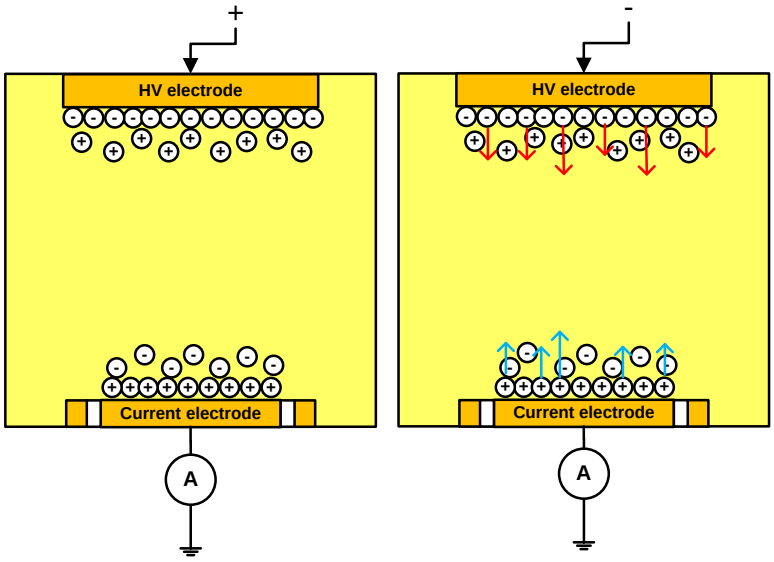

Figure 49. Voltage reversal method for mobility measurement

The voltage reversal method was used for a 1.1 mm gap in the range 5 to 30 V. First a voltage is applied to sweep out the ions from the bulk, Figure 49 left side. After charge accumulation on the electrode surface, suddenly voltage polarity is reversed, Figure 49 right sides. The switching time of the voltage polarity was much faster than the transit time of ions. Reversing the voltage forces the accumulated ions on the electrode surface to move towards the opposite electrode. Mobility is determined by obtaining the time of flight from the current curve developed after voltage reversal. Experimental results showed no dependence on the polarity of the voltage used for sweep out the ions in the bulk of the oil.

- **Mineral oil**

The test result for a 10 V application in a 1.1 mm gap is given in Figure 50 section A represent a time period that +10 V is applied for sweeping out the ions from the gap. In section B current curve after reversing the polarity to -10 V is shown, which provides information about the mobility of negative ions by obtaining the time of flight, i.e. is the time interval of reversing the voltage up to the time that current reach's to its maximum value. As shown in Figure 50, sections C and D are reversing the polarity twice more to get mobility of positive and negative ions.

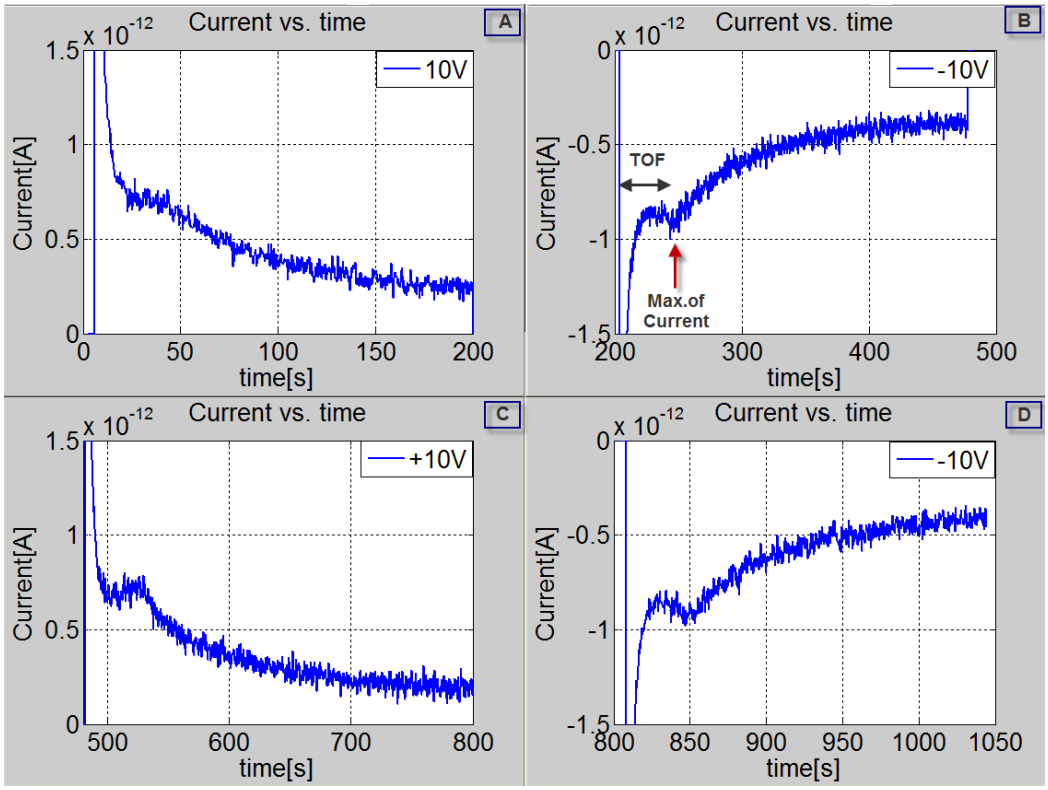

Figure 50. Current curve- Mineral oil - 1.1 mm gap

By knowing the time of flight the mobility can be calculated from equation (28). The results are given in Table 8 in Appendix A. Figure 51 to Figure 54 shows plots of the obtained results. It can be noticed that the mobility of ions in positive and negative for mineral oil is around $2.6 \times 10^{-9}\ \frac{m^2}{Vs}$. The resistivity of the oil from the test cell before starting the measurement was $7\ \mathrm{e}^{12}\ \Omega\mathrm{m}$ at 0.001 Hz and after the measurements was $1.4\ \mathrm{e}^{13}\ \Omega\mathrm{m}$ at 0.001 Hz.

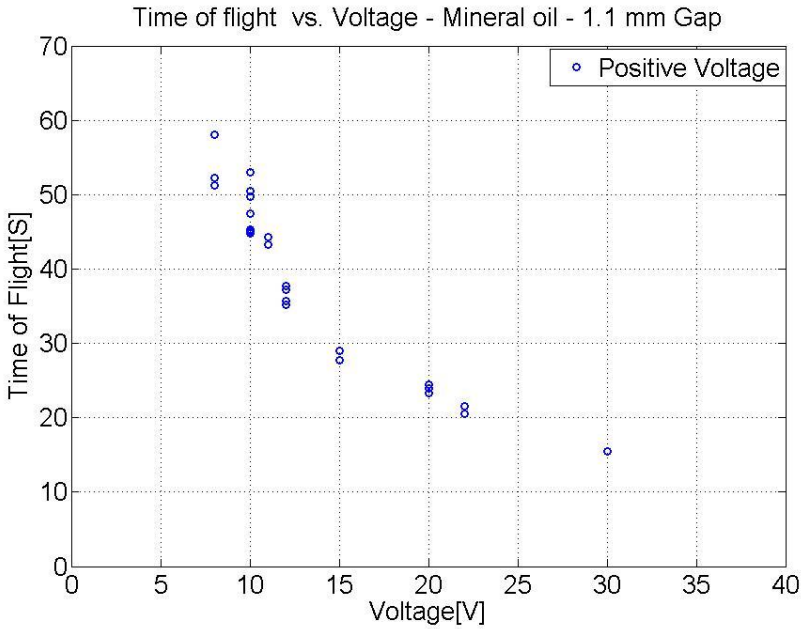

Figure 51. Time of Flight – Mineral oil – Positive Voltage

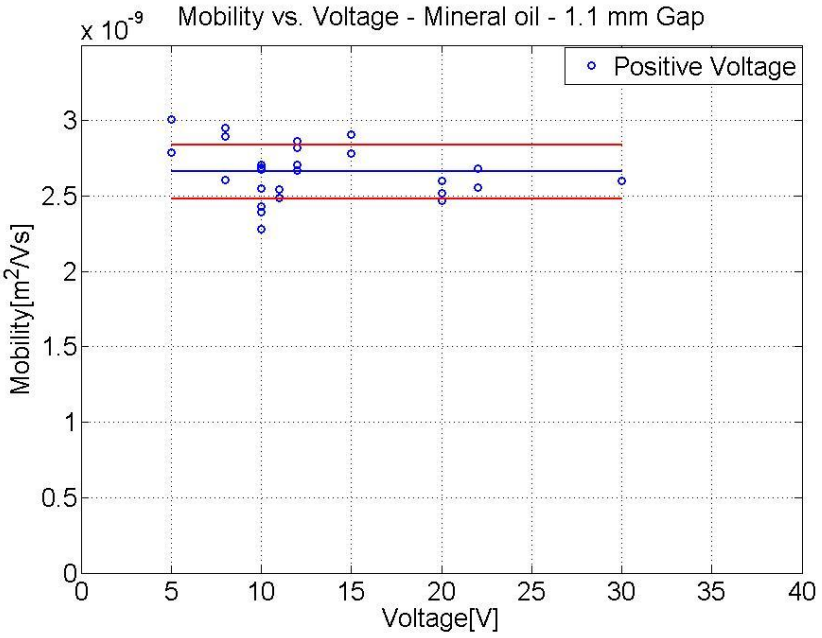

Figure 52. Calculated mobility of positive voltage from TOF – Mineral oil - Blue line is mean value and red lines indicate standard deviation

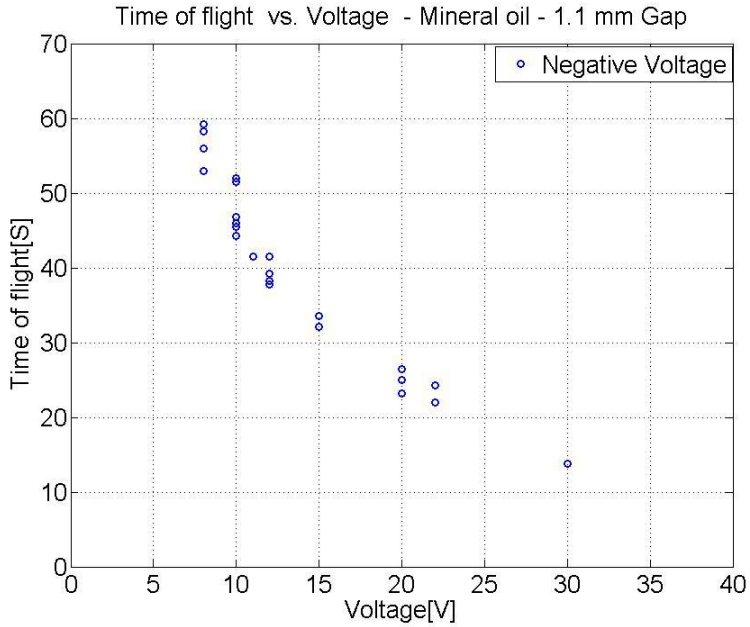

Figure 53. Time of Flight – Mineral oil – Negative voltage

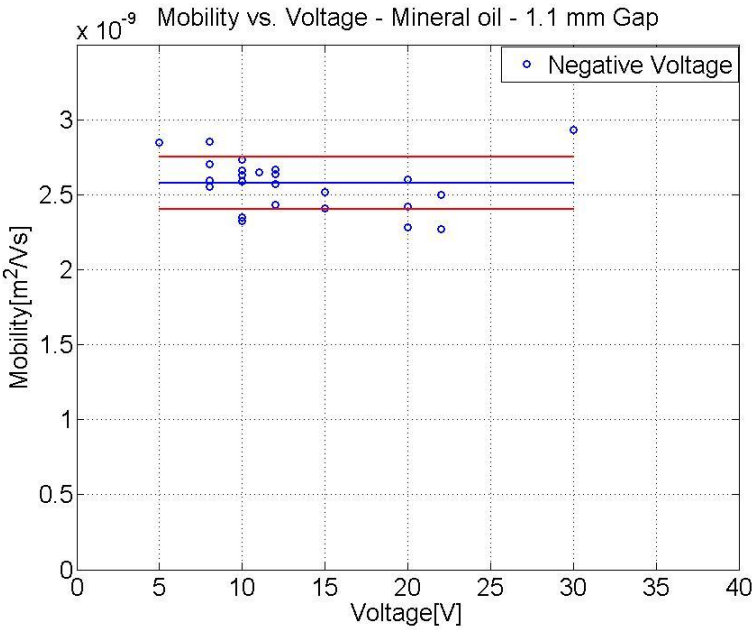

Figure 54. Calculated mobility of negative voltage from TOF – Mineral oil - Blue line is mean value and red lines indicate standard deviation

The blue lines in Figure 52 and Figure 54 are lines of average value of the mobility and red lines are average value plus and minus the standard deviation. For the positive voltage the average value of ion mobility is equal to the $2.66 \times 10^{-9}\ \frac{\mathrm{m}^2}{\mathrm{Vs}}$ and standard deviation is equal to $1.807 \times 10^{-10}\ \frac{\mathrm{m}^2}{\mathrm{Vs}}$. For the negative voltage the average value of ion mobility is equal to the $2.57 \times 10^{-9}\ \frac{\mathrm{m}^2}{\mathrm{Vs}}$ and standard deviation is equal to $1.742 \times 10^{-10}\ \frac{\mathrm{m}^2}{\mathrm{Vs}}$.

According to the experiment results there might be a trend that mobility is the function of the voltage but more data needed to validate this hypothesis.

- **Natural ester oil**

The test cell was cleaned with cyklohexan and filled with non-degassed natural ester oil. Figure 55 shows the result for 1.1 mm gap with 10 V applied. The section A in mentioned figure shows the whole sequence of the test and other sections are zooms of three time intervals. First, negative voltage was applied to sweep out the ions from the gap, section B of Figure 55. After 1000 second, then positive voltage was applied which cause movement of positive ions towards the collecting electrode. After reaching the quasi steady state current, -10 V applied to the high voltage electrode. The mobility of ions in positive voltage application was $1.99 \times 10^{-10}\ \frac{\mathrm{m}^2}{\mathrm{Vs}}$ and for negative voltage was $1.78 \times 10^{-10}\ \frac{\mathrm{m}^2}{\mathrm{Vs}}$.

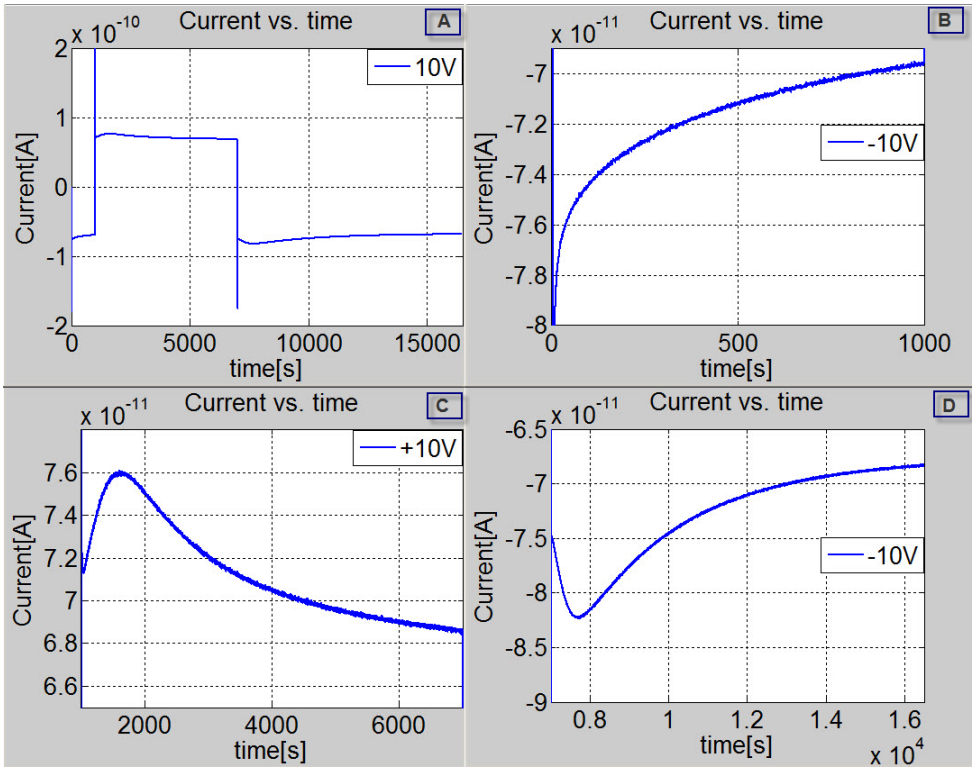

Figure 55. Current curve- Natural ester oil - 1.1 mm gap

Current measurements during voltage reversal show that the initial current with minimal rest time between voltage reversals is within 10 to 20 % of the steady state current which shows that stressing the oil changes its inherent conductivity and that the number of dissociable ion pairs decreases.

The test results with applied 5V are given in Figure 56 and Figure 57. In Figure 56, -5 V was applied for sweeping out the ions from the bulk, section A, and then +5 V was applied.

Mobility of ions in +5V application was equal to: $1.68 \times 10^{-10}\ \frac{m^2}{Vs}$, section B.

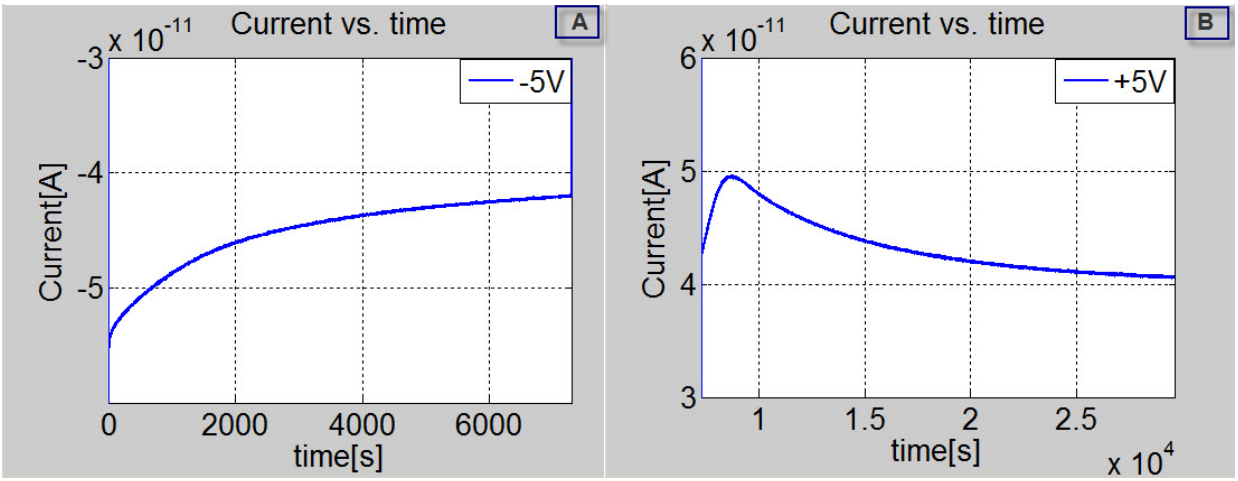

Figure 56. Current curve- Natural ester oil - 1.1 mm gap

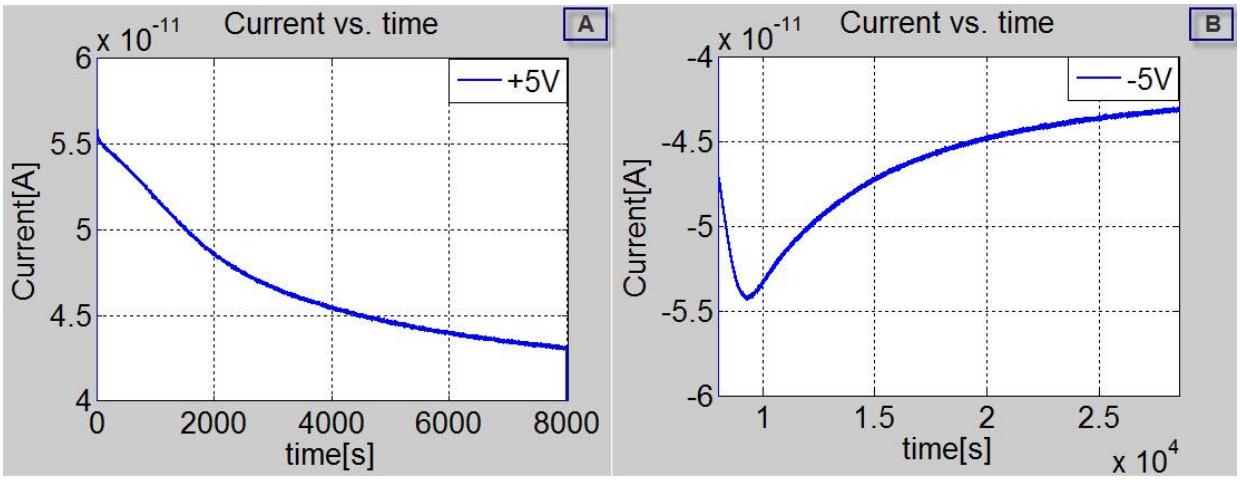

Figure 57. Current curve- Natural ester oil - 1.1 mm gap

In Figure 57, first +5 V was applied to sweep out the ions from the bulk of the oil and then -5 V was applied. Figure 58 to Figure 61provide plots of the result for natural ester oil. It shows that the mobility of ions in positive and negative voltage application in natural ester oil is around, $1.6 \times 10^{-10}\ \frac{m^2}{Vs}$. The results are given in Table 9 in Appendix A.

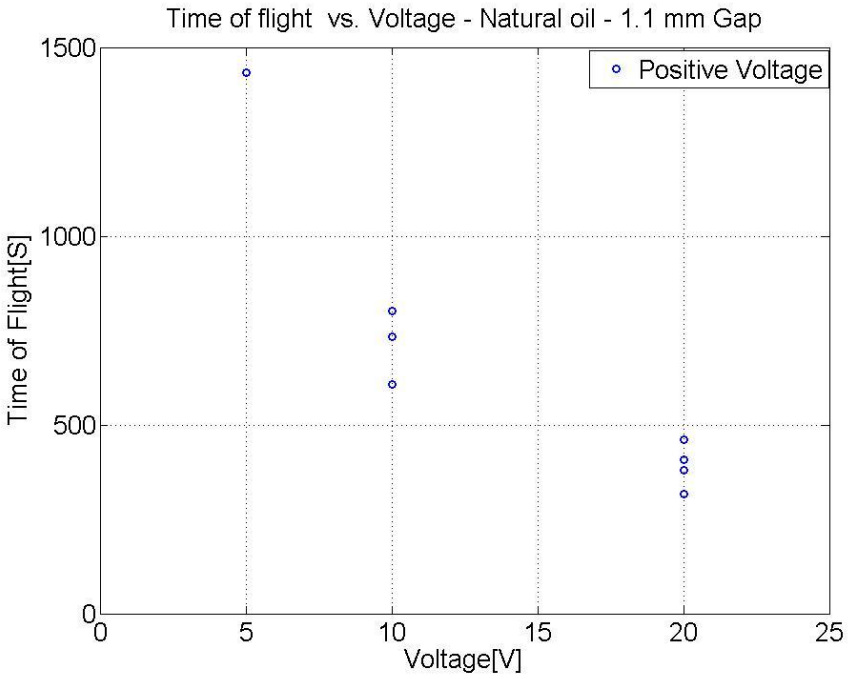

Figure 58. Time of Flight – Natural ester oil – Positive voltage

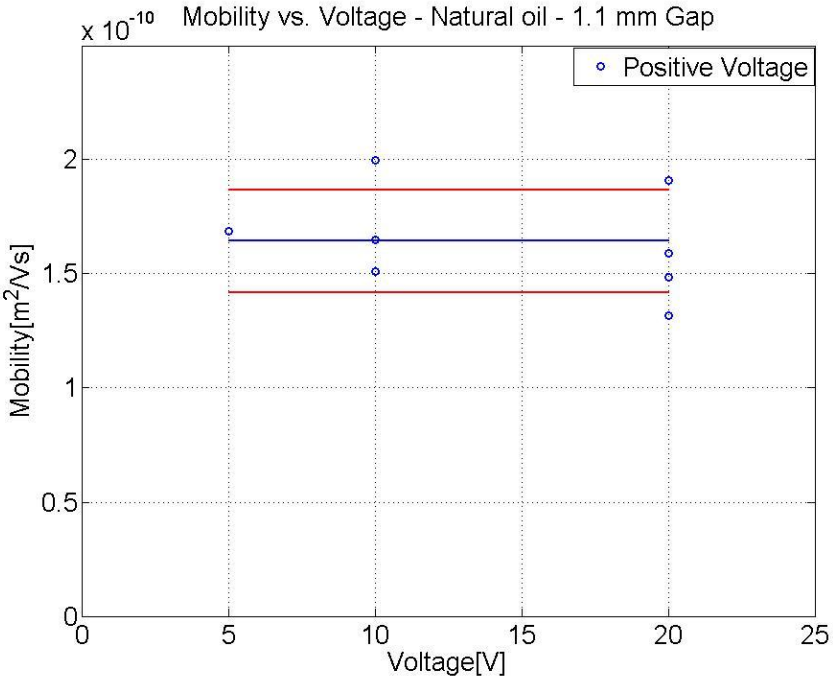

Figure 59. Calculated mobility of positive voltage from TOF – Natural ester oil - Blue line is an average value and red lines indicate standard deviation

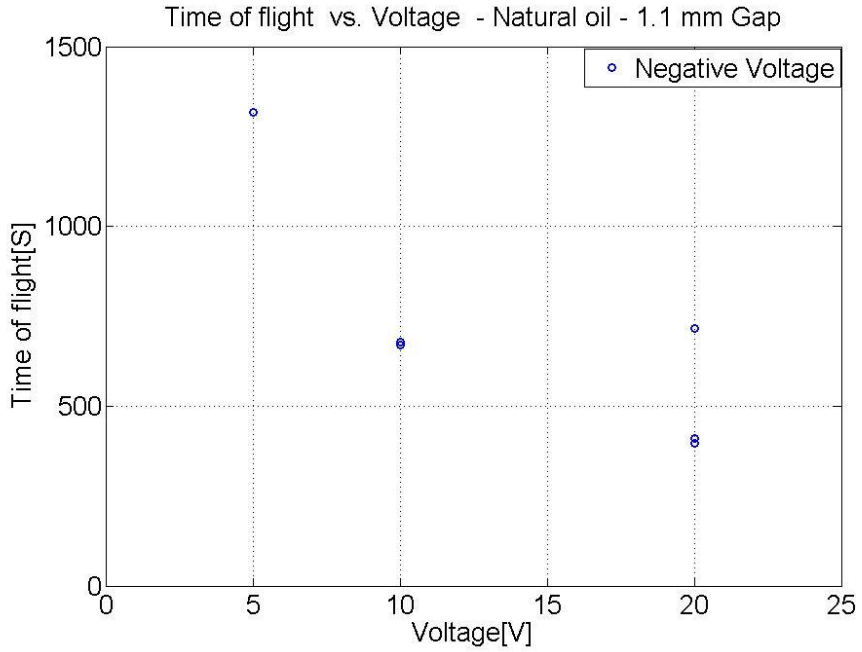

Figure 60. Time of Flight – Natural ester oil – Negative voltage

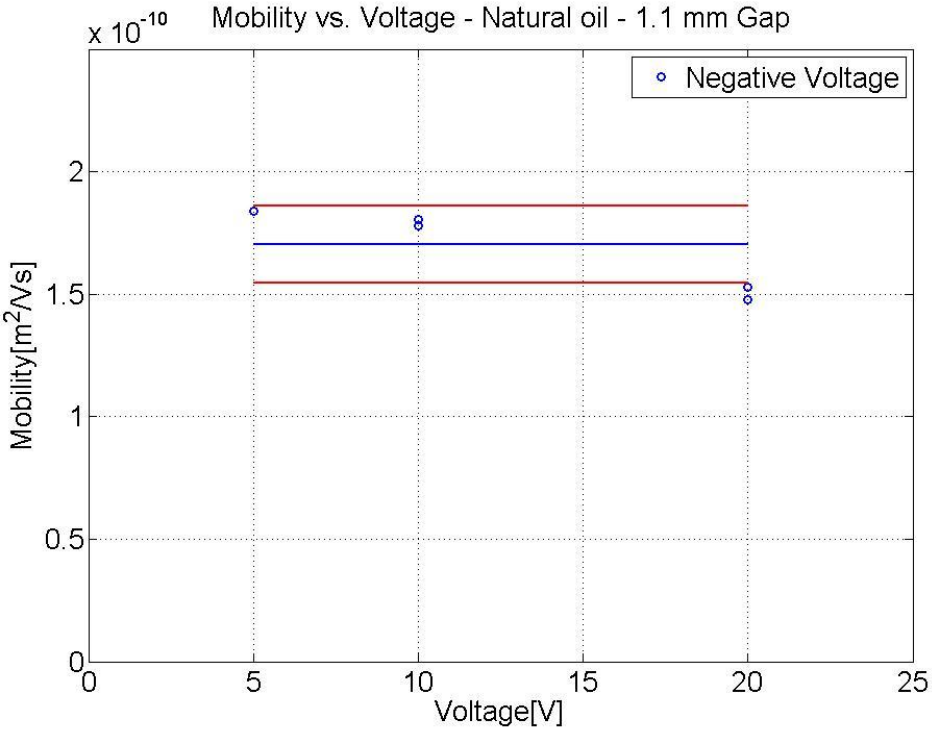

Figure 61. Calculated mobility of negative voltage from TOF – Natural ester oil - Blue line is an average value and red lines indicate standard deviation

The blue lines in Figure 59 and Figure 61 are line of average value of the mobility and red lines are average value plus and minus the standard deviation. For the positive voltage application the average value of ion mobility is equal to the $1.6 \times 10^{-10}\ \frac{\mathrm{m}^2}{\mathrm{Vs}}$ and standard deviation is equal to $2.2 \times 10^{-11}\ \frac{\mathrm{m}^2}{\mathrm{Vs}}$. For the negative voltage application the average value

of ion mobility is equal to the $1.7 \times 10^{-10}\ \frac{\mathrm{m}^2}{\mathrm{Vs}}$ and standard deviation calculated by neglecting the data point in a 20 V application with 718 second time of flight, is equal to $1.6 \times 10^{-11}\ \frac{\mathrm{m}^2}{\mathrm{Vs}}$. The resistivity of the natural ester oil from the test cell before starting the measurement was $6.1\ \mathrm{e}^{11}\ \Omega\mathrm{m}$ at 0.001 Hz. The dielectric relaxation time can be calculated as follow:

$$\tau_{\mathrm{relax}} = \frac{\varepsilon_0\ \varepsilon_{\mathrm{r}}}{\sigma} = \frac{8.854\mathrm{e}^{-12} \times 3.12}{(\frac{1}{6.14\mathrm{e}^{11}})} = 17\ \mathrm{sec}$$

The rest time between each set of tests was sufficiently longer than the dielectric relaxation time.

4.3 RESISTIVITY MEASUREMENTS

The volume resistivity of the oils was determined from current measurement by applying ac voltage. A very low voltage, 2 V, was used for resistivity measurement. Application of higher voltage causes the ions to move out and then the resistivity becomes high. Instruments used for the measurement are listed in a Table 5:

Table 5. Measurement instrument of the resistivity

Type	Model
Measurement system	IDA 200
Measurement cell	IR1
Chamber for measurement	KL1

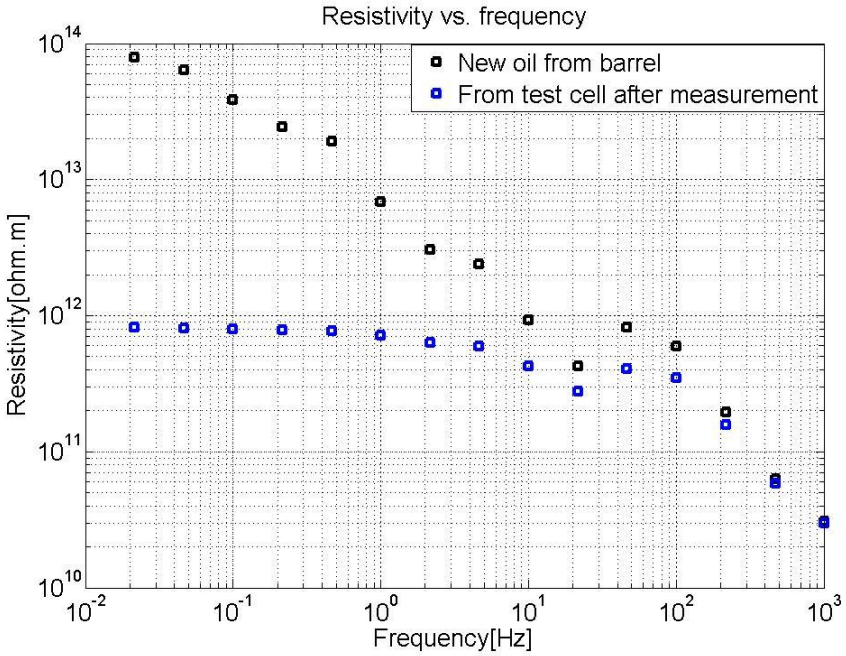

Figure 62. Resistivity of Mineral oil – 5 mm gap

Figure 62 shows the resistivity vs. frequency in a logarithm scale for a mineral oil used in the 5 mm gap experiment. In this figure a black curve is for new oil from the barrel and blue curves are the volume resistivity after finishing the tests.
As it can be seen the resistivity of the oil after measurement is much lower than the value of the resistivity of new oil from the barrel. Another test on new oil from the barrel right after opening showed that the resistivity at 0.001Hz is equal to 2.54 e^{14} Ωm. The difference between the resistivity value before and after measurement can be due to the fact that oil becomes contaminated in the test cell. Previous observation showed that oil resistivity after completion of a test is increased. As it can be seen in Figure 63, the resistivity of the bulk of mineral oil in a 1.1 mm gap test had been increased after doing the measurements. One reason for increasing the resistivity after the tests might be electrostatic cleaning of the oil bulk.
The impurity leads to higher value of the concentration and consequently lower resistivity according to formula (42):

$$\mathcal{R} = \frac{1}{concentration \times mobility \times q} \tag{42}$$

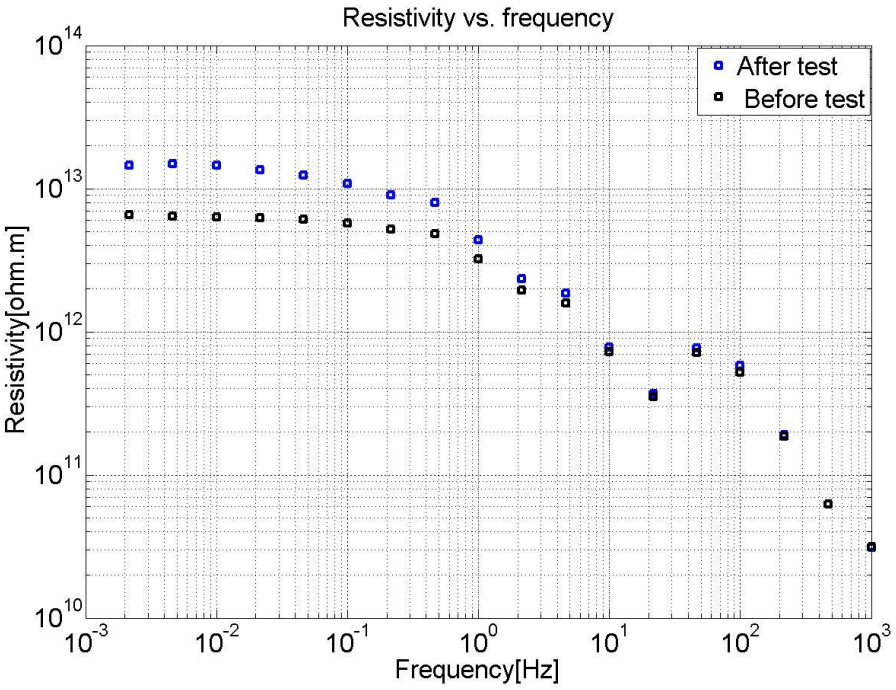

Figure 63. Resistivity of mineral oil – 1.1 mm gap

The bulk resistivity measurement for natural ester oil after doing the test in a 5 mm gap experiment is given in Figure 64. The test on oil from the test cell before starting the measurement in a 1.1 mm gap, showed that the bulk resistivity is equal to $6.17\ e^{11}\ \Omega m$ at 10^{-3} Hz.

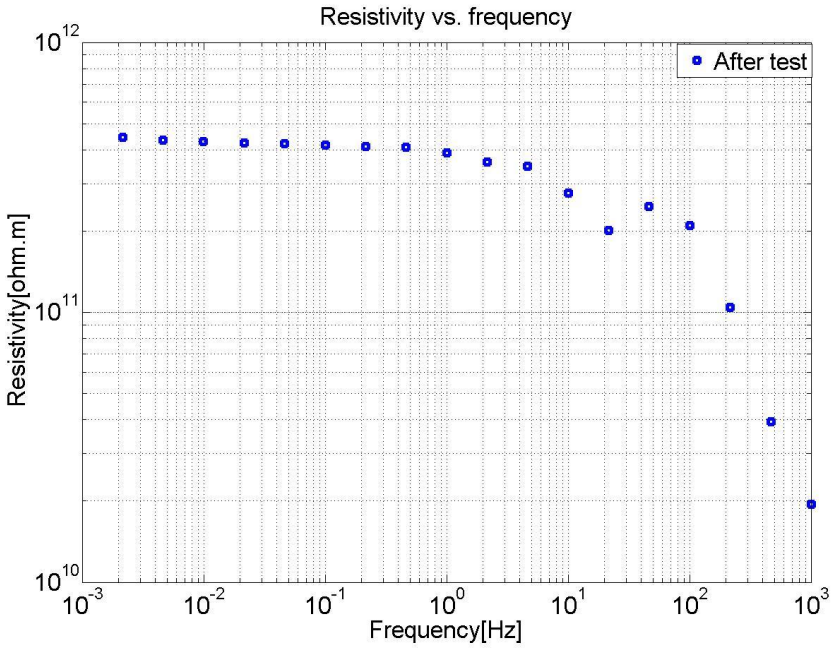

Figure 64. Resistivity of Natural ester oil – 5 mm gap

4.4 Discussion

An investigation had been done to find out the effect of time instant that the polarity of the voltage is reversed, on the ion mobility for natural ester oil. In other words does it make any difference in time of flight if the voltage polarity reversed before the current has reached the steady state or not.

The first test was done on natural oil for a 1.1 mm gap distance. The sequence of the test was similar to the case in Figure 55. First -10 V applied to the high voltage electrode for 1000 second to sweep out the ions from the bulk of the oil and then voltage reversed to 10 V. But in this case, Figure 65, the time interval before final polarity reversal to -10 V was shorter than the case in Figure 55. In Figure 65, the section “A” shows the whole sequence of the experiment and sections “B”, “C” and “D” are zooms of the three time intervals of the experiment. The mobility of ions in positive voltage application calculated from section “C” was $1.73 \times 10^{-10}\ \frac{m^2}{Vs}$ and for negative voltage calculated from section “D” was $3.99 \times 10^{-10}\ \frac{m^2}{Vs}$. This shows that reversing the voltage polarity before reaching to the quasi steady state current leads to quite different mobility of ions for positive and negative voltage application. The mobility of the ions obtained from the current curve after reversing the voltage polarity before reaching to the quasi steady state current, is not the true mobility.

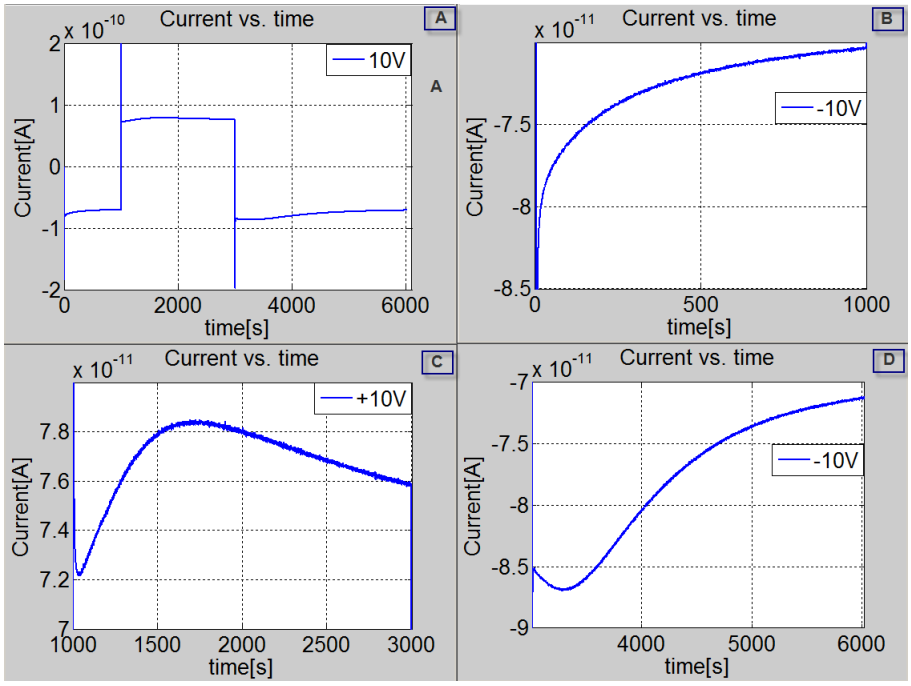

Figure 65. Current curve- Natural ester oil - 1.1 mm gap- shorter time interval

This observation is consistent as the experiment with 20 V shown in Figure 66.

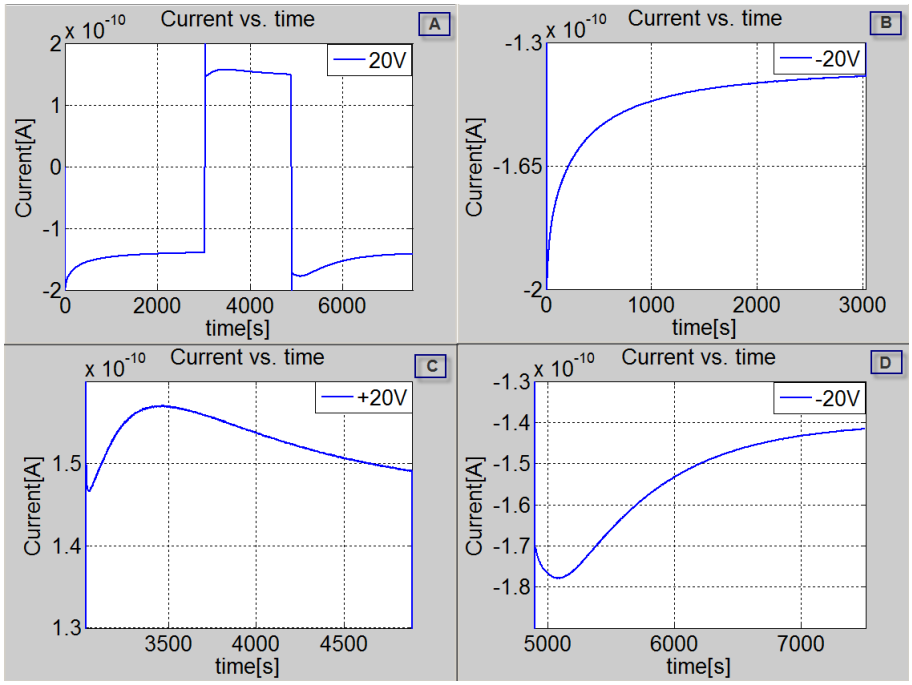

Figure 66. Current curve- Natural ester oil - 1.1 mm gap – Shorter interval

The mobility of ions for positive voltage application calculated from section “C” of Figure 66 is $1.48 \times 10^{-10}\ \frac{m^2}{Vs}$ and mobility of ions in negative voltage application calculated from section “D” by obtaining the time of flight is equal to $3.11 \times 10^{-10}\ \frac{m^2}{Vs}$. The reason of this

phenomenon is may be the fact that longer time interval between voltage reversal will leads to decrease of the reservoir of the ions accumulated near to the electrode surface while if polarity reversal is done before reaching the quasi steady state current there are still ions accumulated on the electrode surface which will contribute to the fast increase of the currents after reversing the voltage polarity. The other reason can be that the small disturbance in homogenous charge distribution near to the electrode surface could trigger filaments followed by turbulent structure which leads to EHD flow even at low voltages. In an equilibrium condition a higher voltage should be applied to see the EHD phenomenon.

The next test had been done to check the effect of longer time intervals on the value of positive and negative mobility, Figure 67. In this case -10 V was applied at the beginning for a longer time comparing to the cases of Figure 55 and Figure 65 and also voltage polarity reversal had been done after longer time period.

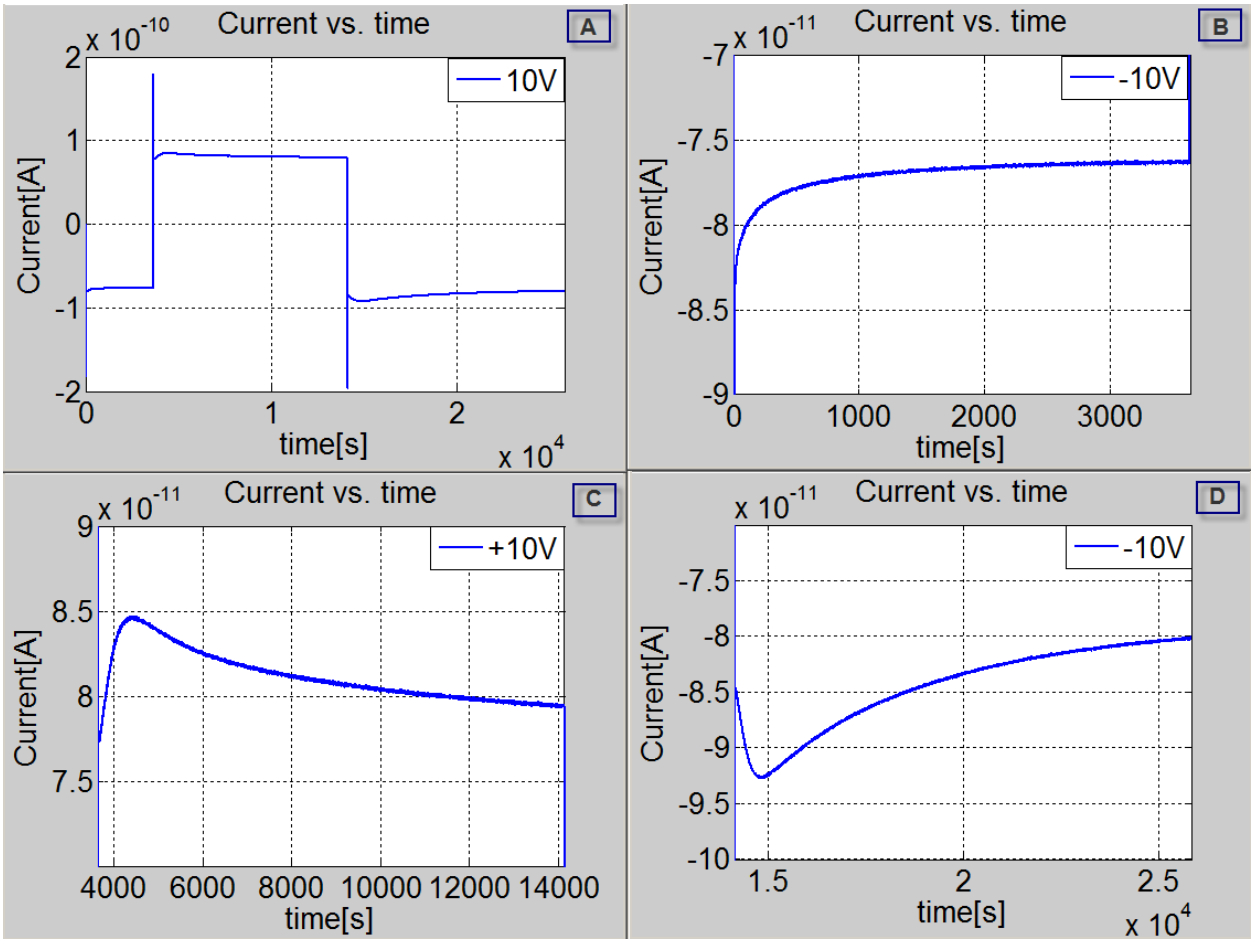

Figure 67. Current curve- Natural ester oil - 1.1 mm gap- Longer time interval

The mobility of ions in when positive voltage applied to high voltage electrode obtained from section “C” was $1.64 \times 10^{-10}\ \frac{\mathrm{m}^2}{\mathrm{Vs}}$ and for negative voltage application calculated from section ”D” was $1.84 \times 10^{-10}\ \frac{\mathrm{m}^2}{\mathrm{V.s}}$. There is not a big difference between the result of this experiment and the experiment of the Figure 55. In order to calculate the mobility of ions in positive and negative voltage polarity, one should wait long enough to reach the quasi steady state current. New series of the test for a mineral oil need to be done with longer time intervals

between voltage polarities reversing. The summary of the experiment result for 10 V is presented in the Table 6.

Table 6. Mobility of the ions with different waiting time before voltage reversal

Short waiting time , 10V	$\mu_+ = 1.73 \times 10^{-10}\ \frac{m^2}{Vs}$	$\mu_- = 3.99 \times 10^{-10}\ \frac{m^2}{Vs}$
Long waiting time, 10 V	$\mu_+ = 1.99 \times 10^{-10}\ \frac{m^2}{Vs}$	$\mu_- = 1.78 \times 10^{-10}\ \frac{m^2}{Vs}$
Short waiting time, 20 V	$\mu_+ = 1.48 \times 10^{-10}\ \frac{m^2}{Vs}$	$\mu_- = 3.11 \times 10^{-10}\ \frac{m^2}{Vs}$
Long waiting time, 20 V	$\mu_+ = 1.31 \times 10^{-10}\ \frac{m^2}{Vs}$	$\mu_- = 1.47 \times 10^{-10}\ \frac{m^2}{Vs}$

Another phenomenon observed in natural oil over a 1.1 mm gap was a small second bump in current curve in a section “C” of Figure 68 for 20 V experiment.

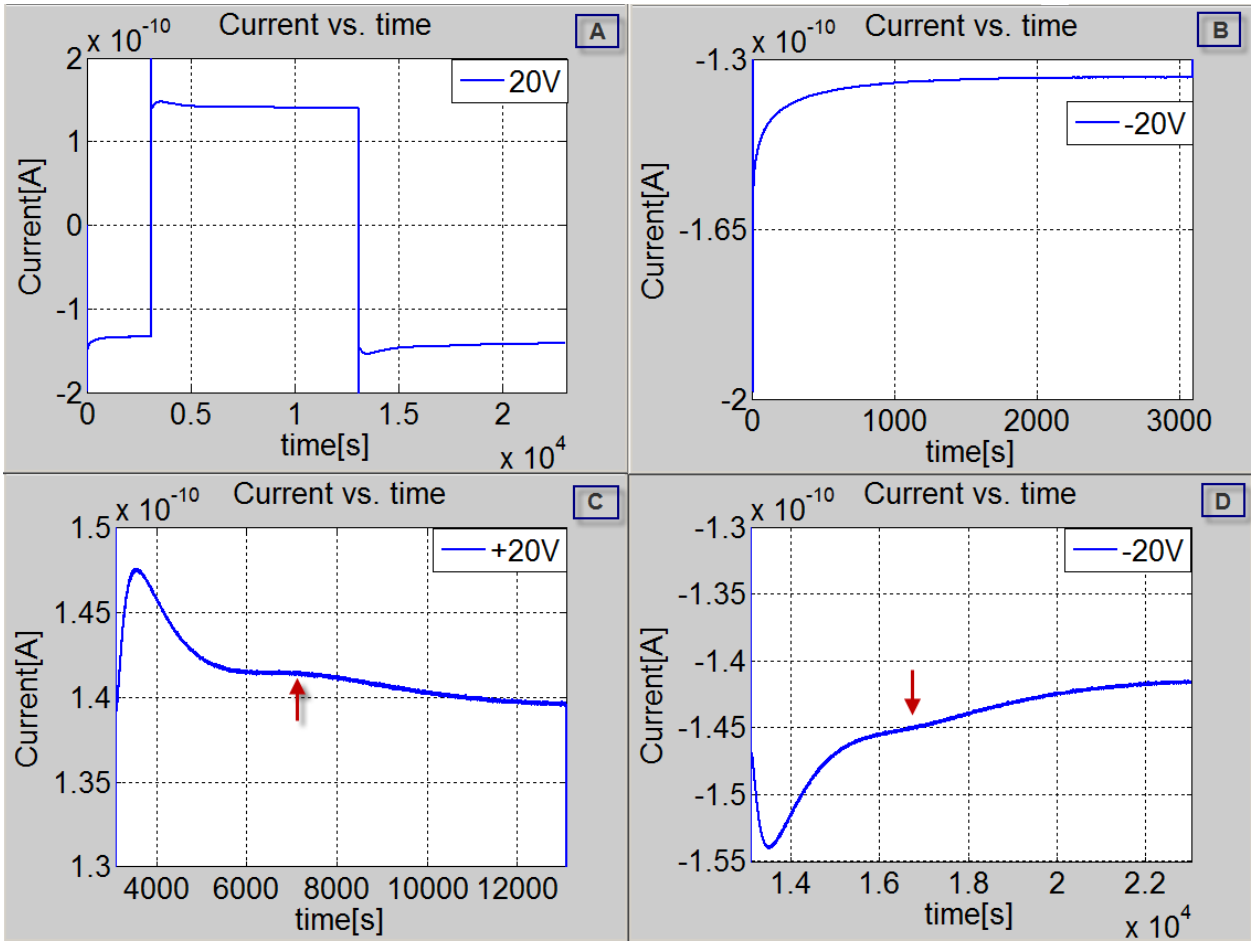

Figure 68. Current curve- Natural ester oil - 1.1 mm gap- Longer time interval

Further investigation need to be done to find out the reason of this so called “second bump” and to check if it is consistent or not because in the experiment with 10 V it had not been

seen, Figure 69. The expected second bump in 10 V test should appear after longer time comparing to 20 V experiment because of longer time of flight in 10 V experiment.
As it was expected, the computer simulation for the voltage reversal showed that the current bump after voltage reversing was much smaller than the current bump for the first application of the voltage. The reason is the outgoing boundary condition at electrode surface.

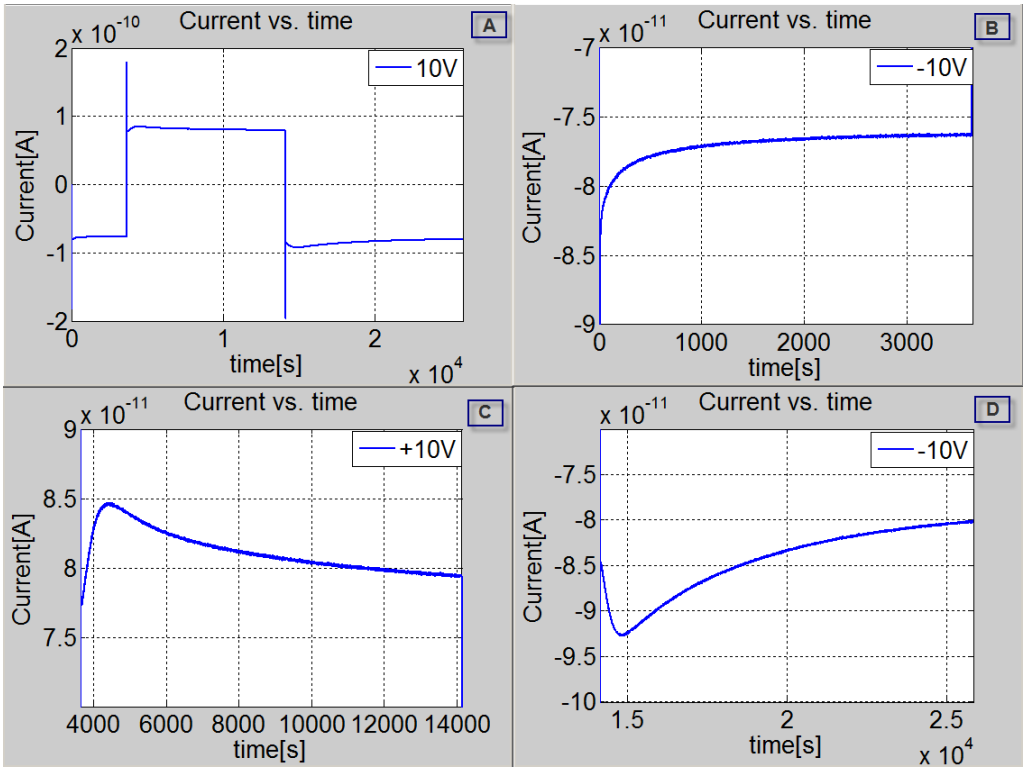

Figure 69. Current curve- Natural ester oil - 1.1 mm gap- Longer time interval

The results indicate that high voltage application causes an EHD flow in the bulk of oil and consequently a higher value of the mobility is obtained, which is in fact the apparent mobility. The impurities in the liquid of industrial quality hampered the study of generation, transport and annihilation of electric charge carriers. The impurity in hydrocarbons consists of water, alcohols and organic acids. Dust particles are other harmful impurities to which ions attach and lead to dramatic change in ionic transport properties [4].
The polar impurities which tend to cluster the ionic core cause a perturbation in ion/liquid interaction. In this study the ion mobility was measured, ignoring if it had cluster of particles around it or not.
The effective radius of moving particle was calculated according to Walden's rule the formula (16). The result is given in a Table 7.

Table 7. Effective radius of the ions

	Viscosity [mm^2/s]	**Mobility[m^2/Vs]**	**Effective radius[m]**
Mineral oil	17	2.55×10^{-9}	1.9×10^{-7}
Natural ester oil	110	1.65×10^{-10}	4.7×10^{-7}

5 CONCLUSIONS AND FUTURE WORK

5.1 Conclusions

Ion mobility in insulation oil has an effect on the dynamics of an electric field distribution in oil gaps. Measurement of positive and negative ion mobility helps to improve accuracy in the simulation of electric field distribution in oil based HVDC insulating system. The plane parallel electrode set-up is suited for the measurement of the ion mobility in a symmetric (constant) electric field. In order to measure the true mobility a low voltage should be applied to avoid EHD cusps. It is important that in a voltage reversal method, the polarity reversal is done after reaching to the quasi steady state current. The mobility of ions in positive and negative voltage application for two types of the transformer oil had been measured in mineral oil and in natural ester oil. The mobility of ions in both positive and negative voltage polarity was almost identical. For mineral oil the measured mobility was around $2.61 \pm 0.175 \times 10^{-9}\ \frac{m^2}{Vs}$ and for natural ester oil was $1.67 \pm 0.18 \times 10^{-10}\ \frac{m^2}{Vs}$ .Previous experiment for a mineral oil showed that the mobility of positive and negative ions are identical and equal to: $1.0 \pm 0.3 \times 10^{-9}\ \frac{\mathrm{m}^2}{\mathrm{Vs}}$ [8].

5.2 Future work

The list of future work is as follow:

- Investigation of the effect of temperature on ion mobility. The temperature will change the viscosity and consequently the mobility value according to Walden's rule.
- Investigation of the effect of age of transformer oil on the mobility.
- Investigating on voltage threshold that yields EHD movement in transformer oil. EHD will cause an increase of true mobility to the apparent mobility.
- Investigation of the effect of acid, water and other impurities on the mobility.
- Investigation of the dependence of current and mobility on the electrode material.
- Development of a more robust data acquisition system.

6 REFERENCES

[1] A,Jaksts and U.Gäfvert; Temporal Development of the Electric Field within a Stressed Oil Gap; IEEE Transaction on Electrical Insulation, Vol.23 No.4, Aug 1988, pp. 723-728

[2] T.Nara, K.kato, F.Endo and H.Okubo; Study on dielectric breakdown at DC polarity reversal in oil/pressboard-composite insulation; 2009 Annual report conference on electrical insulation and dielectric phenomena, pp. 588-591

[3] Uno Gäfvert, Two dimensional measurement of electric fields in transformer oil, ABB Corporate Research Laboratory of Electrical Insulation, pp. 667-671

[4] Werner F. Schmidt; Electrons,Holes,and Ions in Non-Polar Dielectric Liquids;Proceedings of 13th International Conference on Dielectric Liquids (ICDL ’99), Nara,Japan,July 20-25,1999

[5] Uno Gäfvert, et al.; Modeling and measurement of Electric fields in composite oil/cellulose insulation; 2006 Annual report conference on Electrical Insulation and Dielectric Phenomena, pp. 154-157

[6] A.Denat , B. Gosse and J.P.Gosse, Ion injection in hydrocarbons, Laboratoire d’Electrostitque, GRENOBLE Cedex (France),Journal of Electrostatics, 7 (1979), pp. 205-225.

[7] J.O’M. Bockris and A.K.N.Reddy; Modern Electrochemistry 1, Chapter 3, plenum press, New York, 1970

[8] Uno Gäfvert, Albert jaksts, Christer Törnkvist and Lars Walfridsson; Electrical Field Distribution in transformer oil, IEEE Transaction on Electrical insulation, Vol.27 No.3, June 1992, pp. 647-660

[9] A.Alj, A.Denat, J.P.Gosse, B.Gosse and I.Nakamura; Creation of charge carriers in nonpolar liquids; IEEE transaction on electrical insulation Vol.EI-20 No.2, April 1985, pp. 221-231

[10] Internal ABB report

[11] Onsager, Deviations from Ohm’s Law in Weak Electrolytes, J. Chem. Phys.,Vol. 2, 1934, pp. 599-615

[12] Francis o’sullivan, et al.; Modeling the effect of Ionic dissociation on charge transport in transformer oil; 2006 Annual report conference on Electrical Insulation and Dielectric Phenomena, pp. 756-759

[13] J.J.THOMSON, G.P.THOMSON; Conduction of electricity through gases; Cambridge Univ. Press (1928)

[14] A.Denat, B. Gosse, J.P.Gosse; Electrical conduction of solution of an ionic surfactant in hydrocarbons; Journal of Electrostatics, 12 (1982), pp. 197-205

[15] Khrapak A.G., Schmidt W.F; Mobility of simple ions in non-polar dielectric liquids

[16] Anders Åberg, Measurement of charge formation in dielectric liquids in cylindrical geometry, IEEE CEIPD 1994, pp. 790-797

[17] Se-Hee Lee, et al; Finite element analysis of charge injection and transport in dielectric liquid; 2006 Annual report conference on Electrical Insulation and Dielectric Phenomena, pp. 129-132

[18] A.Toureille, G.Touchard,T.Richardson; Electrical double layer at dielectric liquid/solid interface.Space charge measurements using the thermal step methods; IEEE Symposium on Electrical Insulation, June 1996, pp. 758-762

[19] R.Tobazeon, Electrohydrodynamic instabilities and electroconvection in the transient and A.C. regime of unipolar injection in insulating liquids: a review, Journal of electrostatics, 15 (1984), pp. 359-384

[20] M.Nemamcha, J.P.Gosse, B.Gosse and A.Denat; Influence of Insulating Electrode Coating on the Electrical Conduction of Cyclohexane; IEEE transaction on Dielectrics and Electrical Insulation, Vol.23 No.4, Aug 1988, pp. 529-534

[21] P.Atten and J.P.Gosse,J.Chem. Phys., 51 (1969)2804

[22] I. Adamczewski; ioniazation, conductivity and breakdown in dielectric liquids, Taylor & Francis Ltd,London,1969

[23] A.O.Allen, M.P.de Hass and A.Hummel; Measurement of ionic mobilities in dielectric liquids by means of concentric cylindrical electrodes, pp. 2587-2592

[24] P. Atten, Electrohydrodynamic instability and motion induced by injected space charge in insulating liquids, IEEE transaction on Dielectrics and Electrical Insulation, Vol.3 No.1, Feb 1996, pp. 1-17

[25] G.A. Ostroumov, J.Techn.Phys., USSR,24(1954)1915

[26] J.C.Filippini,J.C.Lacroix and R.Tobazeon, Comtes-Rendus Paris,271B(1970) 73 and 936

[27] A.Jaksts, U.Gäfvert; Transient charge injection from blocking electrodes in transformer oil on the reversal of the voltage polarity; Insulation technology ASEA research and innovation

[28] COMSOL Multiphysics Manual, Version 3.5 a

[29] Internal ABB report

[30] Peter S. Winokur, Marvin L.Roush and Joseph Silverman; Ion mobility measurement in Dielectric liquids, J. of Chem. Phys, Vol.63, No.8, 15 Oct 1975, pp. 3478-3489

7 APPENDIX A

7.1 Table of experiment results

7.1.1 Mineral oil – 1.1 mm gap

Table 8. Mineral oil – 1.1 mm gap

Oil type	Voltage	Gap	Electrometer range	Time of flight	Calculated Mobility[$\frac{m^2}{Vs}$]
Mineral oil	+5 V	1.1mm	20 pA	80.5 sec	$3e^{-9}$
Mineral oil	+5 V	1.1mm	20 pA	86.75 sec	$2.78e^{-9}$
Mineral oil	-5 V	1.1mm	20 pA	85 sec	$2.84e^{-9}$
Mineral oil	+8 V	1.1mm	20 pA	58 sec	$2.6e^{-9}$
Mineral oil	+8 V	1.1mm	20 pA	52.25 sec	$2.89e^{-9}$
Mineral oil	+8 V	1.1mm	20 pA	51.25 sec	$2.95e^{-9}$
Mineral oil	+8 V	1.1mm	20 pA	52.25 sec	$2.89e^{-9}$
Mineral oil	-8 V	1.1mm	20 pA	53 sec	$2.85e^{-9}$
Mineral oil	-8 V	1.1mm	20 pA	56 sec	$2.7e^{-9}$
Mineral oil	-8 V	1.1mm	20 pA	59.25 sec	$2.55e^{-9}$
Mineral oil	-8 V	1.1mm	20 pA	58.25 sec	$2.59e^{-9}$
Mineral oil	-10 V	1.1mm	200 pA	51.5 sec	$2.34e^{-9}$
Mineral oil	-10 V	1.1mm	200 pA	52 sec	$2.32e^{-9}$
Mineral oil	-10 V	1.1mm	20 pA	46 sec	$2.63e^{-9}$
Mineral oil	-10 V	1.1mm	20 pA	46 sec	$2.63e^{-9}$
Mineral oil	-10 V	1.1mm	20 pA	46.75 sec	$2.58e^{-9}$
Mineral oil	-10 V	1.1mm	20 pA	44.25 sec	$2.73e^{-9}$
Mineral oil	-10 V	1.1mm	20 pA	45.5 sec	$2.65e^{-9}$
Mineral oil	+10 V	1.1mm	200 pA	53 sec	$2.28e^{-9}$
Mineral oil	+10 V	1.1mm	200 pA	50.5 sec	$2.39e^{-9}$
Mineral oil	+10 V	1.1mm	20 pA	47.5 sec	$2.54e^{-9}$
Mineral oil	+10 V	1.1mm	20 pA	49.75 sec	$2.43e^{-9}$
Mineral oil	+10 V	1.1mm	20 pA	45 sec	$2.68e^{-9}$
Mineral oil	+10 V	1.1mm	20 pA	44.75 sec	$2.73e^{-9}$
Mineral oil	+10 V	1.1mm	20 pA	45.25 sec	$2.67e^{-9}$
Mineral oil	+11 V	1.1mm	20 pA	44.25 sec	$2.48e^{-9}$
Mineral oil	+11 V	1.1mm	20 pA	43.25 sec	$2.54e^{-9}$
Mineral oil	-11 V	1.1mm	20 pA	41.5 sec	$2.65e^{-9}$
Mineral oil	+12 V	1.1mm	20 pA	37.75 sec	$2.67e^{-9}$
Mineral oil	+12 V	1.1mm	20 pA	35.25 sec	$2.86e^{-9}$
Mineral oil	+12 V	1.1mm	20 pA	35.75 sec	$2.82e^{-9}$
Mineral oil	+12 V	1.1mm	20 pA	37.25 sec	$2.7e^{-9}$
Mineral oil	-12 V	1.1mm	20 pA	38.25 sec	$2.63e^{-9}$
Mineral oil	-12 V	1.1mm	20 pA	39.25 sec	$2.56e^{-9}$
Mineral oil	-12 V	1.1mm	20 pA	37.8 sec	$2.66e^{-9}$
Mineral oil	-12 V	1.1mm	20 pA	41.5 sec	$2.45e^{-9}$

Mineral oil	+15 V	1.1mm	20 pA	29 sec	$2.78e^{-9}$
Mineral oil	+15 V	1.1mm	20 pA	27.75 sec	$2.9e^{-9}$
Mineral oil	-15 V	1.1mm	20 pA	32.05 sec	$2.51e^{-9}$
Mineral oil	-15 V	1.1mm	20 pA	33.5 sec	$2.4e^{-9}$
Mineral oil	+20 V	1.1mm	20 pA	24.5 sec	$2.46e^{-9}$
Mineral oil	+20 V	1.1mm	20 pA	24.5 sec	$2.46e^{-9}$
Mineral oil	+20 V	1.1mm	20 pA	24 sec	$2.52e^{-9}$
Mineral oil	+20 V	1.1mm	20 pA	23.25 sec	$2.6e^{-9}$
Mineral oil	-20 V	1.1mm	20 pA	25 sec	$2.42e^{-9}$
Mineral oil	-20 V	1.1mm	20 pA	26.5 sec	$2.28e^{-9}$
Mineral oil	-20 V	1.1mm	20 pA	23.25 sec	$2.6e^{-9}$
Mineral oil	+22 V	1.1mm	20 pA	21.5 sec	$2.55e^{-9}$
Mineral oil	+22 V	1.1mm	20 pA	20.5 sec	$2.68e^{-9}$
Mineral oil	-22 V	1.1mm	20 pA	22 sec	$2.5e^{-9}$
Mineral oil	-22 V	1.1mm	20 pA	24.25 sec	$2.26e^{-9}$
Mineral oil	+30 V	1.1mm	20 pA	15.5 sec	$2.6e^{-9}$
Mineral oil	+30 V	1.1mm	20 pA	15.5 sec	$2.6e^{-9}$
Mineral oil	-30 V	1.1mm	20 pA	13.75 sec	$2.93e^{-9}$

7.1.2 Natural ester oil – 1.1 mm gap

Table 9. Natural ester oil – 1.1 mm gap

Oil type	Voltage	gap	Electrometer range	Time of flight	Calculated Mobility[$\frac{m^2}{Vs}$]
Natural ester oil	+5 V	1.1mm	200 pA	1433.5 sec	$1.68e^{-10}$
Natural ester oil	-5 V	1.1mm	200 pA	1317 sec	$1.83e^{-10}$
Natural ester oil	+10 V	1.1mm	200 pA	606.25 sec	$1.99e^{-10}$
Natural ester oil	+10 V	1.1mm	200 pA	733.25 sec	$1.65e^{-10}$
Natural ester oil	+10 V	1.1mm	200 pA	801.25 sec	$1.51e^{-10}$
Natural ester oil	-10 V	1.1mm	200 pA	679.25 sec	$1.78e^{-10}$
Natural ester oil	-10 V	1.1mm	200 pA	670.5 sec	$1.8e^{-10}$
Natural ester oil	-10 V	1.1mm	200 pA	717.75 sec	$1.68e^{-10}$
Natural ester oil	+20 V	1.1mm	200 pA	316.5 sec	$1.91e^{-10}$
Natural ester oil	+20 V	1.1mm	200 pA	460 sec	$1.31e^{-10}$
Natural ester oil	+20 V	1.1mm	200 pA	407.5 sec	$1.48e^{-10}$
Natural ester oil	+20 V	1.1mm	200 pA	380.5 sec	$1.59e^{-10}$
Natural ester oil	-20 V	1.1mm	200 pA	365.5 sec	$1.65e^{-10}$
Natural ester oil	-20 V	1.1mm	200 pA	409.5 sec	$1.47e^{-10}$
Natural ester oil	-20 V	1.1mm	200 pA	396 sec	$1.52e^{-10}$

7.2 Kinematic viscosity

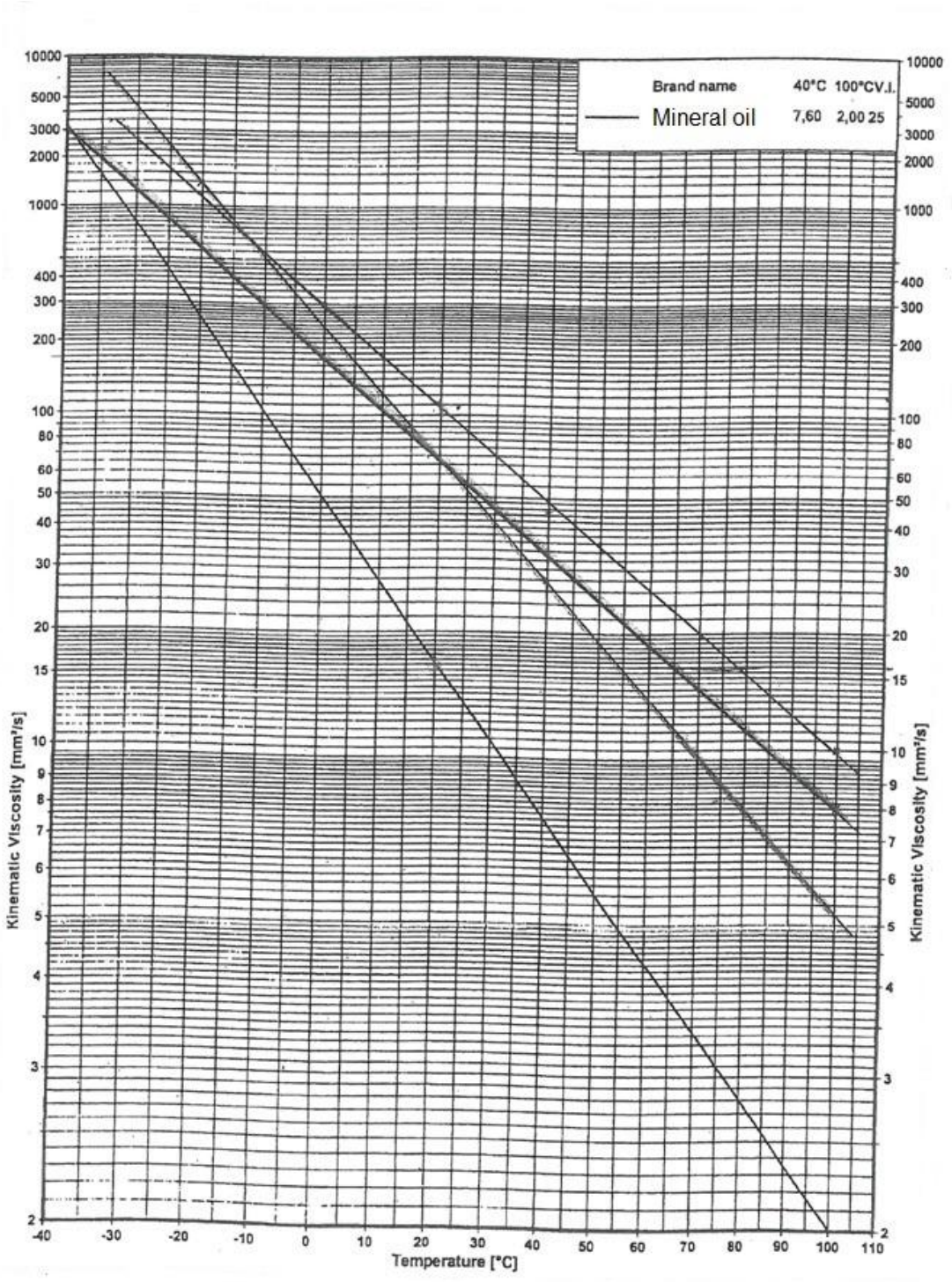

Note: Appendix B is the internal appendix for ABB corporate research.